



34 being discussed involve trapping large amounts of CO<sub>2</sub> as organic carbon in plants or algae and then storing  
35 that carbon in the deep ocean. Here we ask how this type of carbon storage would likely impact the ecology  
36 and chemistry of deep ocean environments, depending on the amount of material placed and its location.  
37 Within the limitations of these first simple calculations, we find that specific anoxic basins like the Black  
38 Sea may have the potential to sequester climatically relevant quantities of organic carbon for more than  
39 1,000 years with moderate changes to deep water chemistry. With these results, it is our aim to motivate  
40 rigorous field and experimental studies that develop more nuanced models for the impacts of carbon storage  
41 in locations like the Black Sea.

42

### 43 **Key Points**

44 Organic carbon sequestration may be relatively efficient in parts of the ocean without O<sub>2</sub>, although its  
45 durability depends on local circulation.

46 The Black Sea may have the potential to durably sequester climatically relevant quantities of organic  
47 carbon.

48 Research is urgently needed to better understand potential biomass degradation rates and the mixing and  
49 transport of degradation products.

50

51

52

53

## 54 **1. Introduction**

55 Both dramatic, rapid CO<sub>2</sub> emissions reduction as well as enhanced atmospheric CO<sub>2</sub> removal are required  
56 to limit average global temperature increases to 2.0 °C or below. This 2.0 °C is considered critical for  
57 avoiding the most severe impacts of climate change (Armstrong McKay et al., 2022; IPCC AR6, 2021).

58 There is therefore a global need to develop a suite of atmospheric CO<sub>2</sub> removal (CDR) techniques that  
59 operate at the gargantuan scale of excess anthropogenic CO<sub>2</sub> emissions – approximately 40 Pg or 40 Gt  
60 CO<sub>2</sub> per year – while minimizing environmental and social risks. Ocean biomass sequestration is one of  
61 the primary CDR strategies discussed in recent strategy reports (National Academies of Science,  
62 Engineering, and Medicine, 2021) and can encompass a wide range of techniques including enhanced  
63 upwelling, seaweed farming, and crop waste sinking, among others. Each of these techniques presents a  
64 distinct suite of potential benefits and risks (Boyd et al., 2022), but there has been minimal research to date

65 into the likely impacts of deep ocean biomass sequestration on the water column and seafloor (c.f., Ocean  
66 Visions and Monterey Bay Aquarium Research Institute, 2022). Deep benthic seafloor ecosystems remain  
67 largely unexplored, and we learn more each year about their complexity and function (Orcutt et al., 2020).  
68 These seafloor environments are sensitive to the changes in geochemical and physical conditions that could  
69 result from biomass storage (Levin et al., 2023) in ways that are likely to vary substantially depending on  
70 local conditions.

71 In this contribution, we investigate the biogeochemical impacts of deep ocean biomass storage on or near  
72 the seafloor, focusing on environments that lack the O<sub>2</sub> required to support a canonical animal community  
73 or aerobic microbial respiration. We discuss differences between the biogeochemical processes that control  
74 the efficiency of organic carbon storage in oxygenated (“oxic”) versus deoxygenated (“anoxic”) environments,  
75 and we present calculations that constrain the potential biogeochemical impacts of biomass  
76 storage in three well-studied anoxic basins on Earth today. We exclude issues related to biomass sourcing  
77 pathways from seaweed farming to land-based agriculture, each of which have their own distinct and  
78 complex issues that require separate attention. Our site-specific approach is intended to be generalizable to  
79 any marine or terrestrial carbon source and to motivate rigorous further rigorous research on these topics.

80

## 81 **2. Background**

### 82 **2.1 Organic carbon sequestration in oxic and anoxic environments**

83 Throughout Earth history, the enhanced burial of organic carbon in seafloor sediments has been one of the  
84 principal mechanisms by which atmospheric CO<sub>2</sub> concentrations have declined from hothouse regimes. The  
85 Ocean Anoxic Events (OAEs) of the Mesozoic provide particularly dramatic examples of this phenomenon  
86 (Schlanger and Jenkyns, 1976; Jarvis et al., 2011; Owens et al., 2018). For example, during the Late  
87 Cretaceous period, atmospheric CO<sub>2</sub> concentrations were near ~1400 ppm (Du Vivier et al., 2015) and a  
88 particularly widespread ocean anoxia event (OAE-2, ~94 million years ago) facilitated the burial of  
89 massive, organic carbon-rich deposits across the proto-North Atlantic (Sinninghe Damsté and Köster, 1998;  
90 Raven et al., 2019) and had global consequences for biodiversity (Bambach, 2006). This 500,000-year-long  
91 burial event, representing an excess organic carbon burial of  $\sim 3 \times 10^{18}$  mol C (132,000 Pg CO<sub>2</sub> at an average  
92 rate of  $\sim 0.26$  Pg CO<sub>2</sub>/yr), drove a global carbon-isotope excursion in the residual marine DIC pool and is  
93 thought to have been so effective at reducing atmospheric CO<sub>2</sub> that it caused the Plenus cold event (Jarvis  
94 et al., 2011; Owens et al., 2016; Kuhnt et al., 2017). In marginal marine environments during OAE-2, local  
95 organic carbon accumulation rates of up to  $2.15 \text{ g cm}^{-2} \text{ kyr}^{-1}$  were nearly 100x higher than modern averages  
96 for similar environments (Raven et al., 2019; Hülse et al., 2021). Although OAE-2 occurred over much

97 longer timescales than are relevant for CDR, it provides valuable insights into the mechanisms of long-term  
98 organic carbon burial that might be leveraged to enhance rates of atmospheric CO<sub>2</sub> removal.

99 Critical environments for carbon burial during OAE-2 and other similar events typically have high  
100 sedimentation rates, elevated local primary productivity, and limited O<sub>2</sub> penetration into sediment  
101 porewaters (Hedges and Keil, 1995; Hartnett et al., 1998; Bianchi et al., 2018). In the absence of O<sub>2</sub>,  
102 microorganisms can respire organic carbon using alternative electron acceptors such as nitrate and sulfate  
103 to break down many organic molecules, although certain (oxidized) molecules can become energetically  
104 inaccessible at low Eh (Boye et al., 2017). Anoxic conditions also limit the functionality of oxidative  
105 exoenzymes that rely on oxygen radicals or O<sub>2</sub> to generate small organic molecules (Sinsabaugh, 2010),  
106 which can be subsequently consumed by single-celled organisms. Microbial sulfate reduction (MSR)  
107 produces sulfide, which can react with (or “sulfurize”) certain functional groups in organic matter (Kohnen  
108 et al., 1990; van Dongen et al., 2006; Raven et al., 2021) and contribute significantly to rates of organic  
109 carbon preservation in sediments (Sinninghe Damsté and Köster, 1998; Raven et al., 2018; Hülse et al.,  
110 2019). Together, these processes supported CO<sub>2</sub> sequestration as organic-rich shales in anoxic basins during  
111 climatically sensitive intervals throughout Earth history and continue to support hotspots of organic carbon  
112 burial today (Bianchi et al., 2018).

113 Another important factor limiting rates of biomass breakdown during OAE-2 and in anoxic basins more  
114 generally is the absence of most eukaryotic organisms, including the vast majority of multicellular grazers.  
115 These organisms physically mix surface sediments and degrade organics, thereby enhancing biomass  
116 breakdown (Aller, 1994; Aller and Cochran, 2019). Although some animals, e.g., nematodes, can survive  
117 periods of anoxia, anoxic conditions preclude growth for all but the most specialized eukaryotes (Fenchel,  
118 2012). Instead, the principal organisms found in these basins are bacteria and archaea. Anaerobic fungi play  
119 a poorly constrained role in anoxic marine environments, but least 18 genera of anaerobic fungi have been  
120 reported so far (Hess et al., 2020), most of which are found in consortia with methanogenic archaea in  
121 animal gut and rumen studies. Of relevance for potential CDR applications, the effective absence of animals  
122 in anoxic environments means that human activities at the seafloor will not directly encounter complex  
123 animal ecosystems (Levin et al., 2023). Although anaerobic microbial ecosystems undoubtedly have  
124 underappreciated diversity and provide ecosystem services for future discovery, eukaryotic organisms like  
125 animals and plants often have greater human cultural significance and regulatory protection, arguably  
126 making their consideration a higher priority.

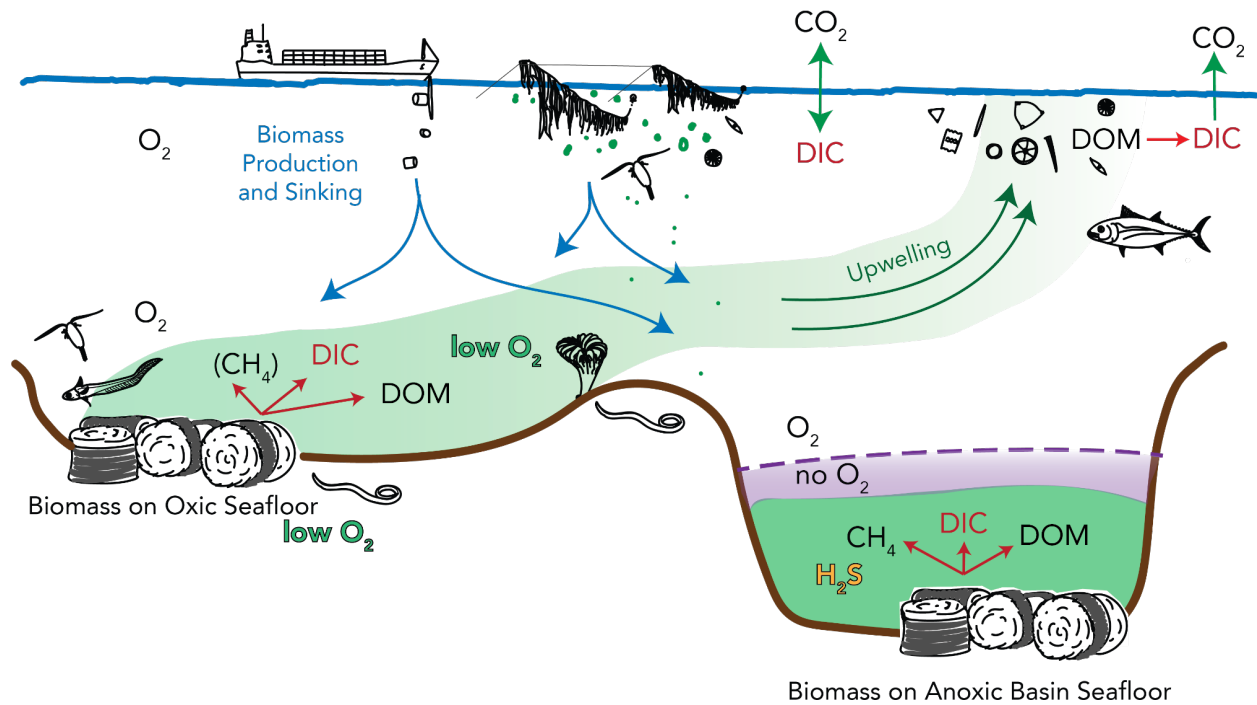
127 Biomass breakdown rates differ for different organic materials, some of which are especially sensitive to  
128 changes in oxygenation and available respiratory metabolisms. Generally speaking, aerobic and anaerobic  
129 microorganisms have the capacity to respire certain highly labile compounds at similar rates (Lee, 1992).

130 However, anaerobic organisms have a limited capacity to metabolize more chemically resistant, recalcitrant  
131 molecules like lignins and other structural polymers (Benner et al., 1986; Cowie and Hedges, 1992; Hulthe  
132 et al., 1998; Marchand et al., 2005). Lignins are relatively oxidized compounds that represent a major  
133 proportion (often 15-35%) of biomass in the woody materials of terrestrial plants (Li et al., 2016). In  
134 sediments, lignins are generally resistant to rapid breakdown because specific steps in their degradation  
135 benefit from oxic exoenzymes and/or physical feeding by metazoans (Marchand et al., 2005).  
136 Demethylation of lignins, or the breakdown of methoxy ( $-OCH_3$ ) side chains, can be achieved aerobically  
137 by some bacteria and fungi but also anaerobically by sulfate-reducing, acetogenic, and fermenting bacteria  
138 as well as some methanogenic archaea (Young and Frazer, 1987; Mayumi et al., 2016). Rates of lignin  
139 degradation in anoxic marine systems are generally difficult to detect (Benner et al., 1984; Keil et al., 2010)  
140 and woody (lignin-rich) archaeological remains are famously well-preserved in the Black Sea (Ballard et  
141 al., 2001). Therefore, biomass that is rich in lignins and other oxidized structural polymers is likely to be  
142 especially resistant to biological breakdown under anoxic conditions. In order to maximize the efficiency  
143 of carbon storage in CDR applications, it will be essential to consider the lability of biomass materials under  
144 site-specific conditions and to balance that efficiency against the full life-cycle and environmental impacts  
145 of a particular CDR pathway.

146

## 147 **2.2 Impacts of enhanced organic carbon addition to the seafloor**

148 Delivering large quantities of organic carbon to the seafloor for CDR may impact benthic environments,  
149 the mid-water column, and ‘downstream’ regions such as upwelling zones (Siegel et al., 2021; Levin et al.,  
150 2023; **Fig. 1**). Most of these risks stem from the breakdown of sequestered biomass by heterotrophic  
151 organisms to generate dissolved species, including dissolved organic matter (DOM),  $CO_2$  from respiration,  
152 or the products of anaerobic metabolisms like sulfide ( $H_2S$ ) and methane ( $CH_4$ ). Each of these species can  
153 impact downstream environments or modify the efficiency of carbon storage.  $CO_2$  addition is a source of  
154 acidity and its carbon can be returned to the atmosphere if the host water mass returns to the surface (Siegel  
155 et al., 2021). Remineralized nutrients (e.g., ammonium,  $NH_4^+$ ) may enhance productivity in downstream  
156 (surface) environments or drive changes in expressed anaerobic microbial metabolisms. The release of  
157 DOM, depending on its composition, can stimulate bacterial communities and change the local ecological  
158 structure (Boyd et al., 2022). DOM may also be a future source of  $CO_2$  as it continues to degrade (Sexton  
159 et al., 2011; Paine et al., 2021). Anaerobic microorganisms that remineralize biomass in the absence of  $O_2$   
160 generate alkalinity, methane, reactive metals, and/or sulfide as well as  $CO_2$  and DOM. After their release,  
161 these dissolved compounds will be transported away from seafloor installations by the general circulation  
162 around the sequestration site.



163

164 **Fig. 1. Overview of potential outcomes for organic carbon sequestered in oxic and anoxic regions of**  
 165 **the seafloor.** Red arrows indicate potential pathways for sequestered biomass transformations in the  
 166 environment: respiration to dissolved inorganic carbon (DIC), fermentation to DIC and methane (CH<sub>4</sub>), or  
 167 breakdown to dissolved organic matter (DOM). Organic matter respiration in oxic environments consumes  
 168 O<sub>2</sub>, while OM respiration in anoxic environments generally consumes sulfate (SO<sub>4</sub>) and releases sulfide  
 169 (H<sub>2</sub>S). In the open ocean, dissolved species return to the ocean surface on the timescales of ocean mixing  
 170 (hundreds to thousands of years).

171

172 In sediments, degradation of overlying OM will cause biogeochemical effects that are similar to those seen  
 173 in the water column, but these effects are more locally concentrated near the sequestration site. Organic  
 174 matter accumulations will deplete electron acceptors in sediments, driving them toward more reducing  
 175 conditions (Froelich et al., 1979) and causing bacterial and archaeal heterotrophic communities to adjust to  
 176 favor anaerobic metabolisms. Seafloor communities may also be impacted by the introduction of epibiotic  
 177 organisms, viruses, or chemical species carried in with biomass materials (Fraser et al., 2011). Locally  
 178 elevated concentrations of organic matter may also attract opportunistic scavengers to feed on the deposit.  
 179 The scale and severity of ecological effects will depend on the seafloor region selected for storage.

180 The effects of any CDR strategy on the deep ocean environment will need to be balanced against the  
 181 effectiveness of that approach for removing CO<sub>2</sub> from the atmosphere and marginally reducing climatic  
 182 havoc. The effectiveness of organic matter sequestration in the deep ocean depends on both storage

183 efficiency– the proportion of biomass that resists breakdown on a chosen timescale (section 2.1) – and the  
184 durability of atmospheric CO<sub>2</sub> removal – the timescale on which CO<sub>2</sub> is kept out of the atmosphere in any  
185 form (organic matter, DIC, DOM, or dissolved methane). The durability of marine biomass CDR is strongly  
186 dependent on the depth and downstream circulation of its storage location (**Fig. 1**). Relatively shallow water  
187 masses often upwell back to the surface and release any produced CO<sub>2</sub> on timescales of decades to hundreds  
188 of years. In contrast, packaged and ballasted or otherwise densified organic materials that are effectively  
189 stationary on the abyssal (>2,000 m depth) seafloor will encounter water masses that generally return to the  
190 surface and ventilate their CO<sub>2</sub> more slowly, over hundreds to thousands of years (Siegel et al., 2021).

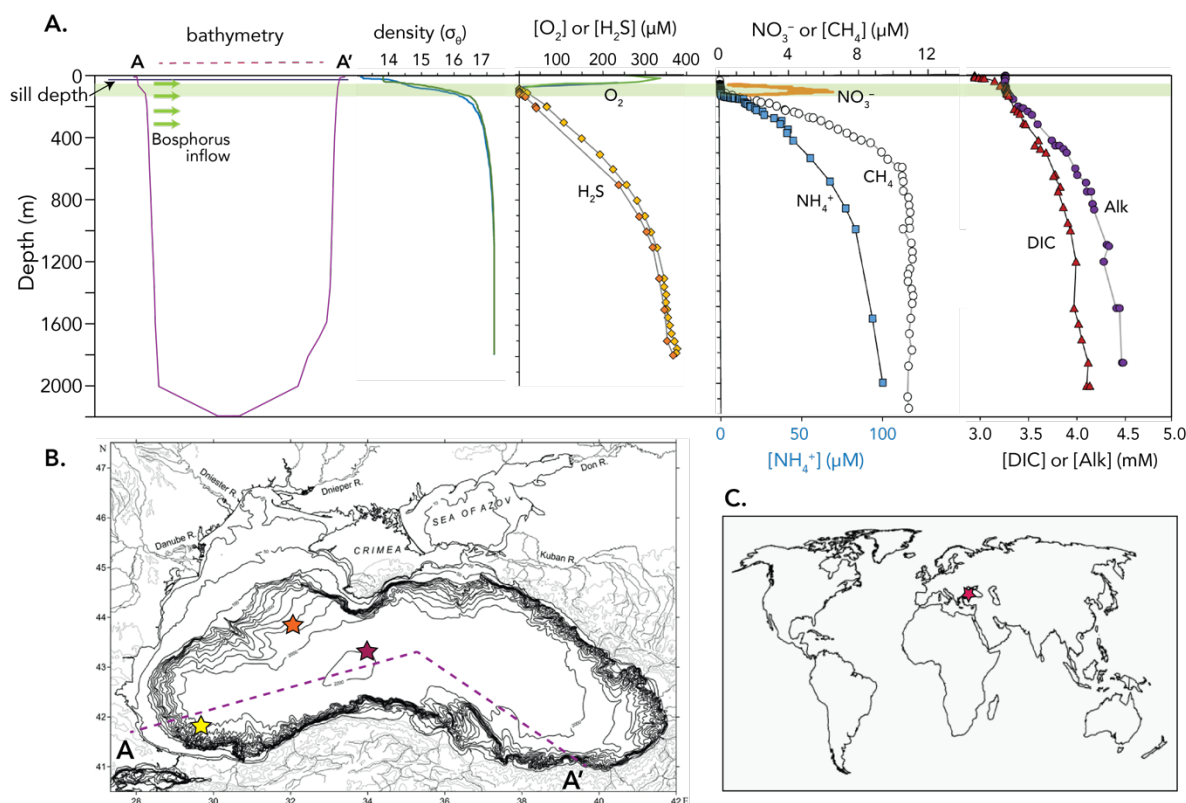
191 Below, we evaluate the potential impacts of biomass respiration on the biogeochemistry of deep anoxic  
192 basins, focusing on cycles of carbon (CO<sub>2</sub> and CH<sub>4</sub>), sulfur (SO<sub>4</sub><sup>2-</sup> and H<sub>2</sub>S), nitrogen (NH<sub>4</sub><sup>+</sup> and NO<sub>3</sub><sup>-</sup>),  
193 phosphate, alkalinity, and pH to inform a preliminary assessment of biogeochemical impacts and ecological  
194 risks. Using published estimates of basin circulation and mixing parameters, we also assess the durability  
195 of storage for dissolved biomass breakdown products in specific basins and estimate the timescales over  
196 which dissolved species may impact the upper water column. Finally, we discuss the potential capacity for  
197 major anoxic basins on Earth today – the Black Sea, Cariaco Basin, and Orca Basin – to sequester organic  
198 carbon at climatically meaningful scales.

199

200

## 201 2.3 Site Description: Modern anoxic basins

### 202 2.3.1 *Black Sea*



203

204 **Fig. 2: Modern geochemical conditions in the Black Sea water column.** (A.) Compiled literature data  
 205 for the Black Sea. Circulation from Murray et al. (1991) and Ivanov and Samadurov (2001); density from  
 206 Konovalov and Murray (2001) and Dubinin et al. (2022);  $[O_2]$  from Wakeham et al. (2003) and Dubinin et  
 207 al. (2022);  $[H_2S]$  from Dubinin et al. (2022);  $[NO_3^-]$  and  $[NH_4^+]$  from Konovalov et al. (2006);  $[CH_4]$  from  
 208 Reeburgh et al. (1991); [DIC] and Alk from Hiscock and Millero (2006). Results for nitrogen species, DIC,  
 209 and Alk were converted from  $\sigma_\theta$  units to approximate depth based on the density profiles and alignment in  
 210 Dubinin et al., 2022). (B.) Map showing Black Sea bathymetry. Sampling locations are shown for methane  
 211 (purple star), DIC and Alk (yellow star), and all other station samples (red star). Cross-section A–A' is 1120  
 212 km long. (C.) Global overview map showing the location of the Black Sea as a red star.

213

214 The Black Sea is a vast sulfidic basin covering 322,367 km<sup>2</sup> in eastern Europe, with its ownership divided  
 215 among Turkey, Romania, Bulgaria, Georgia, Russia, and Ukraine (**Fig. 2**). The Black Sea is unique in the  
 216 modern world in terms of its biogeochemistry and scale. Its only connection to the global ocean comes from  
 217 the Mediterranean via the Sea of Marmara and the Bosphorus straits, where the sill is just ~35 m deep. The  
 218 Black Sea became salty approximately 7,100 yrs ago, when rising sea levels after the last deglaciation  
 219 brought Mediterranean seawater over the sill of the Bosphorus straits and into the basin (Ryan et al., 1997),  
 220 leading to the development of a strong density stratification. Today, inflowing seawater mixes with some

221 amount of Black Sea water and sinks to fill the basin, mostly at intermediate depths (<700 m). The Black  
222 Sea receives freshwater inflows from several major rivers, mostly in its northwest, and has a positive water  
223 balance overall. The abyssal Black Sea is characterized by a relatively well-mixed benthic boundary layer  
224 below ~1750 m water depth (Murray et al., 1991). Water movement and density homogenization within the  
225 deep boundary layer are driven by thermal convection (Ivanov and Samodurov, 2001), while mixing within  
226 the mid-water column is driven primarily by mesoscale cyclonic and occasional anticyclonic eddies  
227 (Markova, 2023). Currents in the deep Black Sea thus differ from the well-known rim current system in  
228 surface water.

229 The combination of density stratification and high surface productivity leads to the depletion of O<sub>2</sub> below  
230 ~80 m water depth and the accumulation of sulfide below ~100-130 m water depth. Due to its long residence  
231 time in the deep basin (~2,000 yrs, Lee et al., 2002), deep (>2,000 m) water in the Black Sea is relatively  
232 acidic (pH ~7.4) and has accumulated large amounts of DIC (4,100 μM), ammonia (100 μM), phosphate  
233 (10 μM), alkalinity (4,400 μM), silica (350 μM) and DOC (0.5 mM) (Hiscock and Millero, 2006) (**Fig. 2**).  
234 Sulfide concentrations in the deep basin have varied over time, with reported values ranging from 350– 440  
235 μM (Konovalov and Murray, 2001; Hiscock and Millero, 2006; Dubinin et al., 2022). Sulfide is a major  
236 contributor to the total alkalinity budget in the deep Black Sea (Hiscock and Millero, 2006).

237 Especially since the mid-20<sup>th</sup>-century, the biogeochemistry of the Black Sea has been substantially impacted  
238 by eutrophication, which provides an illustrative example of how the basin responds to changes in organic  
239 matter flux. Between the 1960s and 1980s, enormous fluxes of agricultural nutrients drove a more-than-  
240 doubling of primary productivity in the central Black Sea (Konovalov and Murray, 2001). This excess  
241 organic carbon was largely remineralized in the upper water column by oxic respiration and, after the  
242 depletion of available O<sub>2</sub>, via MSR, which produces sulfide. Eutrophication over this period has caused  
243 sulfide production in the basin to roughly double, adding 0.13-0.22 Tmol excess H<sub>2</sub>S/yr (Konovalov and  
244 Murray, 2001). This substantial perturbation to the upper water column led to an apparent shoaling of both  
245 the upper and lower interfaces of the sub-oxic zone (Konovalov 2001).

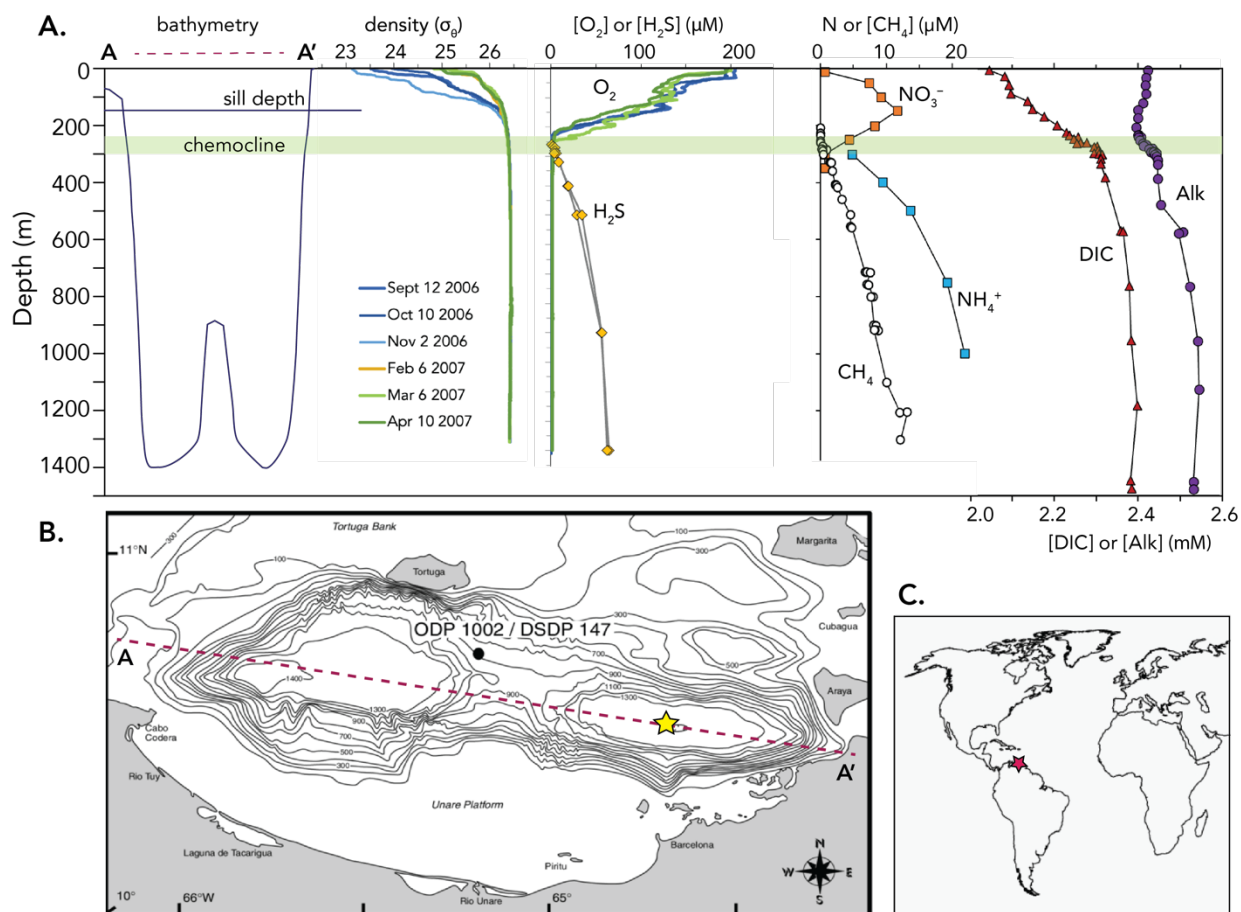
246 At moderate depths and especially near the shallow northwestern shelf, fluxes of organic matter to the  
247 sediments of roughly 0.47 Tmol of organic carbon/yr (Dubinin et al., 2022) are often sufficient to exhaust  
248 dissolved sulfate in pore water and drive methanogenesis (Reeburgh et al., 1991; Jørgensen et al., 2001).  
249 Sediments from the shelf and slope in the Black Sea therefore produce substantial amounts of methane,  
250 releasing ~0.29 Tmol CH<sub>4</sub>/yr to the basin, while abyssal sediments are thought to be sinks for methane  
251 overall (Reeburgh 1991). Methane is also injected into the basin from point sources like seeps and methane  
252 ‘volcanoes,’ which are concentrated at depths below 750 m. Total methane sources from seeps and other  
253 point sources are estimated to be ~0.39 Tmol CH<sub>4</sub>/yr (Schmale et al., 2011), but less than 1% of this methane

254 reaches the atmosphere due to a combination of slow mixing and active anaerobic oxidation of methane  
 255 (AOM) in the anaerobic water column ( $\sim 6 \mu\text{M CH}_4/\text{yr}$ ) (Wakeham et al., 2003; Starostenko et al., 2010;  
 256 Egorov et al., 2011; Schmale et al., 2011). Water column methane concentrations are  $\sim 11 \mu\text{M}$  below 500  
 257 m and 10 nM at the surface (**Fig. 2**).

258

259 **2.3.2 Cariaco Basin**

260 The Cariaco Basin is a 200-km-by-50-km trench located on the Venezuelan continental shelf that is  
 261 separated from the Caribbean Sea by a sill at  $\sim 150$  m water depth. Since roughly the end of the last glacial  
 262 period, restricted circulation in the 1400 m-deep basin and high surface productivity have caused the basin  
 263 water to be sulfidic below  $\sim 350$  m depth. Cariaco Basin was the focus of an international long-term time  
 264 series program from 1995 to 2017 (Muller-Karger et al., 2019), which provides a high-resolution record of  
 265 the relationship between upwelling and productivity in the basin.



266

267 **Fig. 3: Cariaco Basin geochemistry.** (A.) Compiled literature data for Cariaco Basin. Density and  $[\text{O}_2]$   
 268 from the CARIACO time series database (<http://imars.marine.usf.edu/CAR/>);  $[\text{H}_2\text{S}]$  from Li et al. (2010);

269  $[\text{NO}_3^-]$  and  $[\text{NH}_4^+]$  from Thunell et al. (2004);  $[\text{CH}_4]$  from Scranton et al (1988);  $[\text{DIC}]$  and  $[\text{Alk}]$  from  
270 Hastings and Emerson (1988). (B.) Map showing Cariaco Basin bathymetry. The yellow star indicates the  
271 location of the CARIACO long-term time series station and profile site for all data except DIC/Alk. The  
272 cross-section A–A' is 200 km long. (C.) Global overview map showing the location of Cariaco Basin as a  
273 red star.

274 Cariaco Basin is more weakly stratified than the Black Sea and experiences seasonal upwelling (Muller-  
275 Karger et al., 2004). The density gradient in the water column (**Fig. 3**) is driven entirely by a small  
276 temperature differential from  $\sim 18.1^\circ\text{C}$  at the surface to  $\sim 16.8^\circ\text{C}$  at depth, while deep water is less saline  
277 than surface water. Accordingly, eddy diffusion coefficients in eastern Cariaco Basin (Scranton et al., 1987)  
278 are  $\sim 30\times$  higher than those measured in the Black Sea, which means that dissolved components mix toward  
279 the chemocline on much faster timescales. This temperature gradient is also not always stable, as Scranton  
280 et al. (1987) noted significant warming from 1955-1982 and the basin may have experienced a full overturn  
281 in the early 20<sup>th</sup> century (Zhang and Millero, 1993). Accordingly, concentrations of sulfide in the deep basin  
282 do not appear to be in steady-state and may be reset by tectonic activity and associated periodic intrusions  
283 of oxygenated seawater (Scranton et al., 2001).

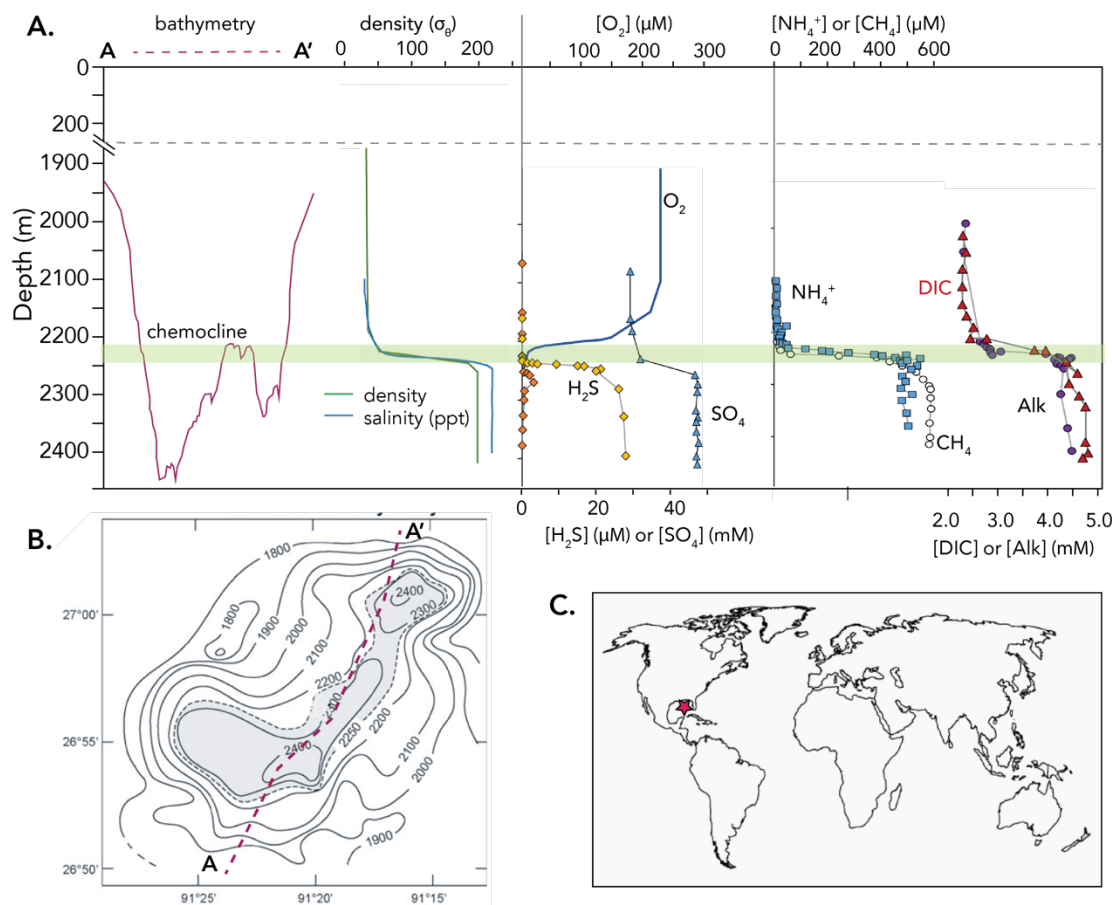
284 Upwelling in the region drives elevated productivity and organic carbon export to the basin of about  $\sim 1\times 10^{11}$   
285 g C/yr (0.008 Tmol C/yr). In the sulfidic water column, most of this organic matter is respired via sulfate  
286 reduction. In the sediments, estimated methane fluxes of roughly  $10 \mu\text{mol cm}^{-2} \text{ yr}^{-1}$  (Scranton, 1988)  
287 suggests that at least 25% of the carbon delivered to sediments each year ( $75\text{-}80 \mu\text{mol cm}^{-2} \text{ yr}^{-1}$ ; Muller-  
288 Karger et al., 2004) is eventually consumed via methanogenesis, while 35% is consumed by sulfate  
289 reduction and  $\sim 40\%$  is preserved (Raven et al., 2016). Although a total of nearly  $7.1\times 10^8 \text{ mol CH}_4 \text{ yr}^{-1}$  is  
290 produced in Cariaco sediments, roughly  $\sim 85\%$  of this methane is oxidized in the anoxic water column  
291 (Reeburgh, 1976; Scranton, 1988). In the deep basin, the approximately linear increase in methane  
292 concentrations to  $\sim 10 \mu\text{M}$  is thought to primarily reflect methane sourced from the sediments (**Fig. 3**; Ward  
293 et al., 1987; Scranton, 1988).

294

### 295 2.3.3 *Orca Basin*

296 Orca Basin is a 200-meter-deep seafloor depression filled with anoxic, hypersaline water that underlies  
297  $\sim 2,200$  meters of 'normal' oxygenated seawater in the Gulf of Mexico. The continental shelf bordering  
298 Louisiana and Texas (USA) is pockmarked by many such basins, generally produced by the intersection of  
299 tectonics and salt dissolution. The total volume of brine in Orca Basin is  $\sim 10.24 \text{ km}^3$ , and the basin area at

300 the permanent halocline is 158 km<sup>2</sup> (Diercks et al., 2019). Brines have been isolated from overlying  
 301 seawater for at least 7,900 years (Addy and Behrens, 1990).



302  
 303 **Fig. 4: Orca Basin geochemistry.** (A.) Compiled literature data for Orca Basin. Bathymetry based on  
 304 seismic reflection profiles from Shokes et al. (1977); density from Millero et al. (1979); salinity from Van  
 305 Cappellen et al. (1998);  $[O_2]$  from Trefry et al. (1984);  $[H_2S]$  from Wiesenberg et al. (1984) and Van  
 306 Cappellen et al. (1998);  $[NH_4^+]$  and  $[Alk]$  from Van Cappellen et al. (1998),  $[CH_4]$  from Wiesenberg et al.  
 307 (1984),  $[DIC]$  from Sackett et al. (1979). (B.) Map modified from Tribovillard et al. (2009). The grey shaded  
 308 area on the map corresponds to the lateral extent of the brine. The cross-section A–A' is approximately 28  
 309 km long. (C.) Global overview map showing the location of Orca Basin as a red star.

310  
 311 Seawater in Orca Basin is extraordinarily salty (47–318 psu; 258 g/kg; Shokes et al., 1977) due to  
 312 dissolution of an exposed salt layer on its north and southeast rims. Brines have been accumulating in the  
 313 basin due to their very high densities ( $\sim 1300$  g/L) for thousands of years (Addy and Behrens, 1980). The  
 314 pycnocline at the top of the brine sits at 2220–2250 m depth and acts as a strong impediment to mixing in

315 either direction. Sinking marine particles and materials transported from the Mississippi are suspended at  
316 this interface, where they age and become substantially degraded (Trefry, 1984; Tribovillard et al., 2008;  
317 Diercks et al., 2019). Organic materials that do eventually sink into the dense brine produce OC-rich soupy  
318 muds that continue to be degraded slowly by sulfate-reducing and methanogenic microorganisms (LaRock  
319 et al., 1979; Hurtgen et al., 1999; Nigro et al., 2020).

320 Due to this long, gradual accumulation of OM breakdown products, Orca Basin brines are rich in DOM  
321 (89-278  $\mu\text{M}$  or  $2.5 \times 10^9$  mol C total; Diercks et al., 2019). Sulfate concentrations are high throughout the  
322 basin and exceed 40 mM in porewater throughout the upper 30 cm of sediments (Hurtgen et al., 1999).  
323 Although microbial sulfate reduction is active in the basin, iron concentrations are high and react efficiently  
324 with sulfide to generate iron monosulfides. Reported concentrations of dissolved sulfides differ; maximum  
325 concentrations of 2-3  $\mu\text{M}$  were reported within a narrow layer within the water column at ~2270 m depth  
326 during two cruises in the late 1970s (Wiesenburg et al., 1985), while Van Cappellen et al. (1998) reported  
327 10 to 28  $\mu\text{M}$  sulfide in all samples with salinities above 200 ppm. Microbes use iron and manganese oxides  
328 in the upper pycnocline at 2200-2240 m depth (Van Cappellen et al., 1998), and iron sulfides precipitate at  
329 the interface between regions of active iron and sulfur cycling (Sheu and Presley, 1986).

330 Despite high concentrations of available sulfate and the observation that hypersaline conditions do not  
331 appear to limit MSR (Porter et al., 2007), methanogenesis is an active pathway of OM breakdown in the  
332 Orca Basin. Methanogens in this environment appear to use 'non-competitive' methylated substrates for  
333 methylotrophic methanogenesis, producing  $^{13}\text{C}$ -depleted methane concurrent with MSR (Zhuang et al.,  
334 2016). Methane and other biogenic hydrocarbons accumulate to high concentrations (up to 3.4 mM  $\text{CH}_4$ )  
335 within the brine (Wiesenburg et al., 1985; Zhuang et al., 2016). Most of this methane is trapped by the lack  
336 of mixing across the pycnocline, but methane that does mix into overlying waters is likely to be oxidized  
337 by microbial communities in the overlying oxic waters of the Gulf of Mexico, which appear to be highly  
338 effective at methane oxidation and are primed from abundant petroleum seep sources (Kessler et al., 2011).

339

### 340 **3. Methods**

#### 341 **3.1 Organic matter stoichiometry**

342 We calculate the geochemical impacts of biomass breakdown in the Black Sea, Cariaco Basin, and Orca  
343 Basin by mixing breakdown products into the abyssal volume of each site and calculating carbonate system  
344 parameters. Conceptually, this calculation evaluates a range of magnitudes for a single hypothetical  
345 sequestration event, assuming that most remineralization occurs immediately thereafter. This first simple  
346 approach has no time-dependence and does not include sinks for any released compounds (e.g., sulfide

347 oxidation). Instead, it constrains the scale of the peak acute perturbation implied by biomass breakdown at  
 348 scale given basin geochemical conditions.

349 We apply a range of stoichiometries for organic matter breakdown that represent end-member compositions  
 350 for carbohydrate-rich and lipid-rich biomass (Redfield, 1934; Anderson and Sarmiento, 1994), with and  
 351 without ammonium reoxidation to nitrate (Hastings and Emerson, 1988). In terms of their impacts on pH,  
 352 DIC, alkalinity, and sulfide, terrestrial biomass sources are approximated by the carbohydrate-rich end  
 353 member; terrestrial materials with lower N:C ratios would have smaller changes in  $\text{NH}_4^+$  concentration than  
 354 these estimates. We first consider a case in which all biomass breakdown occurs via microbial sulfate  
 355 reduction (MSR), which oxidizes biomass to  $\text{CO}_2$  and nutrients while reducing sulfate to sulfide. Unlike  
 356 oxic respiration, microbial sulfate reduction is a source of alkalinity, so its impact on pH is relatively small  
 357 (Lyons et al., 1984). However, the precise ratio of total alkalinity (TA) to DIC produced during organic  
 358 matter remineralization depends on the identity of the organic electron donor and its oxidation state  
 359 (Gallagher et al., 2012); more reduced organic compounds like lipids ( $\sim\text{CH}_2$ ) require more oxidizing power  
 360 to generate  $\text{CO}_2$  than more oxidized compounds like carbohydrates ( $\sim\text{CH}_2\text{O}$ ). We convert widely used  
 361 literature estimates for  $\Delta\text{CO}_2 : \Delta\text{O}_2$  into ratios of  $\Delta\text{CO}_2 : \Delta\text{SO}_4$  ratios by balancing electrons for each half  
 362 reaction (Froelich et al., 1979; Middelburg et al., 2020). We also consider a case in which methanogenesis  
 363 accounts for 10% of total organic C remineralization. In our simplified model, methanogenesis converts  
 364 organic C to methane ( $\text{CH}_4$ ) and  $\text{CO}_2$  in a ratio that depends on the oxidation state of the organic C. This  
 365 reaction does not produce alkalinity and therefore, in the absence of anaerobic methane reoxidation, has a  
 366 relatively large effect on local pH. We present this full range of stoichiometries and metabolisms based on  
 367 five scenarios (Table 1).

	Scenario	Organic Matter	Breakdown Products	$\Delta\text{DIC} :$ $\Delta\text{Alk}$
1	Lipid-rich OM breakdown via MSR	$\text{C}_{117}\text{N}_{16}\text{P}$	$117\text{CO}_2 + 16\text{NH}_4^+ + \text{H}_2\text{PO}_4^- + 85\text{H}_2\text{S}$	+117:+170 (1:1.45)
2	Carb-rich OM breakdown via MSR with ammonium ox.	$\text{C}_{106}\text{N}_{16}\text{O}_{42}\text{H}_{175}\text{P}$	$106\text{CO}_2 + 16\text{NO}_3^- + \text{H}_2\text{PO}_4^- + 69\text{H}_2\text{S}$	+106:+122 (1:1.15)
3	Carb-rich OM breakdown via MSR without ammonium ox.	$\text{C}_{106}\text{N}_{16}\text{O}_{42}\text{H}_{175}\text{P}$	$106\text{CO}_2 + 16\text{NH}_4^+ + \text{H}_2\text{PO}_4^- + 53\text{H}_2\text{S}$	+106:+106 (1:1)
4	Lipid-rich OM breakdown via methanogenesis	$\text{C}_{117}\text{N}_{16}\text{P}$	$32\text{CO}_2 + 85\text{CH}_4 + 16\text{NH}_4^+ + \text{H}_2\text{PO}_4^-$	+32:+1
5	Carb-rich OM breakdown via methanogenesis	$\text{C}_{106}\text{N}_{16}\text{O}_{42}\text{H}_{175}\text{P}$	$53\text{CO}_2 + 53\text{CH}_4 + 16\text{NH}_4^+ + \text{H}_2\text{PO}_4^-$	+53:+1

368 **Table 1.** Reaction stoichiometries used for organic matter compositions and breakdown pathways.  
 369 Balanced reactions linking organic matter to its products require H<sub>2</sub>O and H<sup>+</sup> (not shown). OM = organic  
 370 matter; MSR = microbial sulfate reduction.

371

372 All pH calculations were conducted using CO2SYS v.2.3, which accounts for sulfide, ammonia, and silicic  
 373 acid alkalinity. Conditions in Orca Basin brine exceed calibration limits for carbon system parameters, so  
 374 we did not calculate pH or carbonate solubility change for this site. Our analysis includes the linked cycles  
 375 of carbon, nitrogen, phosphorus, sulfur, and alkalinity, but it excludes any interactions with iron or  
 376 manganese cycling and the effects of organic acids.

377 Basin volumes were calculated in MATLAB R2018B using the trapz function at the 1 arcsecond resolution  
 378 specified in the GEBCO 2022 bathymetry. In the abyssal Black Sea, although vertical mixing is relatively  
 379 well constrained, very little data has been collected relevant to lateral mixing (Stanev et al., 2021).  
 380 Therefore, as a first calculation, we focus only on the western portion of the Black Sea, and we mix the  
 381 products of microbial reactions into a volume equivalent to 43% of the benthic boundary layer between  
 382 1750 m and the seafloor (Murray et al., 1991) to account for these uncertainties in lateral mixing. For  
 383 Cariaco Basin, we calculated the volume of water in the eastern and western sub-basins separately as well  
 384 as the overlying seawater to 350 m, following observed concentration patterns in (Scranton et al., 2001).  
 385 For Orca Basin, products are mixed into a total brine volume of 10.3 km<sup>3</sup> (Diercks et al., 2019). The vertical  
 386 mixing rates within Orca Basin brine have not yet been measured directly.

387

### 388 3.2 Circulation Model

389 Dissolved products of biomass breakdown will not be confined to the deepest layers of the water column.  
 390 For the Black Sea and Cariaco Basin, we use published estimates for advective flow and eddy (turbulent)  
 391 diffusivity to estimate vertical mixing and transport. In each case, we constructed a model composed of 0.1-  
 392 km-thick, vertically stacked layers following Scranton et al. (1987) and Schmale et al. (2011). The general  
 393 equation for this calculation is:

$$394 \quad d[C]/dt = K_i * ([C]_{i-1} - [C]_i) * A_i / (V_i * \Delta z_i) + K_{i+1} * ([C]_{i+1} - [C]_i) * A_i / (V_i * \Delta z_i) + T_B * ([C]_B - [C]_i) / V_i$$

395 where [C] represents the concentration of any component, the subscript 'i' refers to a depth box, T  
 396 represents advective flow in km<sup>3</sup>/yr across the box boundary, z is box thickness (0.1 km), A and V are the  
 397 area and volumes of each box boundary in km<sup>2</sup> and km<sup>3</sup> respectively, and K is eddy diffusivity in km<sup>2</sup>/yr.

398 In the deep Black Sea, estimates for eddy (turbulent) diffusivity are lower than for most open-ocean sites,  
399 ranging from  $4.1 \times 10^{-4}$  to  $1.2 \times 10^{-4}$  km<sup>2</sup>/yr, equivalent to  $4 \times 10^{-6}$  to  $1.3 \times 10^{-5}$  m<sup>3</sup>/sec (Ivanov and Samodurov,  
400 2001). The box model for the Black Sea uses 20 vertically-stacked, 0.1-km-thick layers (Schmale et al.,  
401 2011) to evaluate the timescales over which dissolved products of deep biomass respiration might impact  
402 the upper water column of the Black Sea. Below ~500 m depth in the Black Sea, transport is generally  
403 limited to turbulent diffusion ( $K_i$ ). In the upper 500 m, each box receives advective flow from the Bosphorus  
404 with return via upwelling ( $T_B$ ) and outflow from the surface box (Schmale et al., 2011). The model is run  
405 with a one-year timestep for 1,200 years.

406 In Cariaco Basin, intermittent upwelling and a weak density gradient lead to higher estimates of eddy  
407 turbulent diffusivity than for the Black Sea, ranging from  $1.3 \times 10^{-2}$  to  $2.7 \times 10^{-3}$  km<sup>2</sup>/yr (Scranton et al., 1987).  
408 The box model for Cariaco Basin uses 12 vertically-stacked, 0.1-km-thick layers and is run with 12 time  
409 steps per year for 200 years.

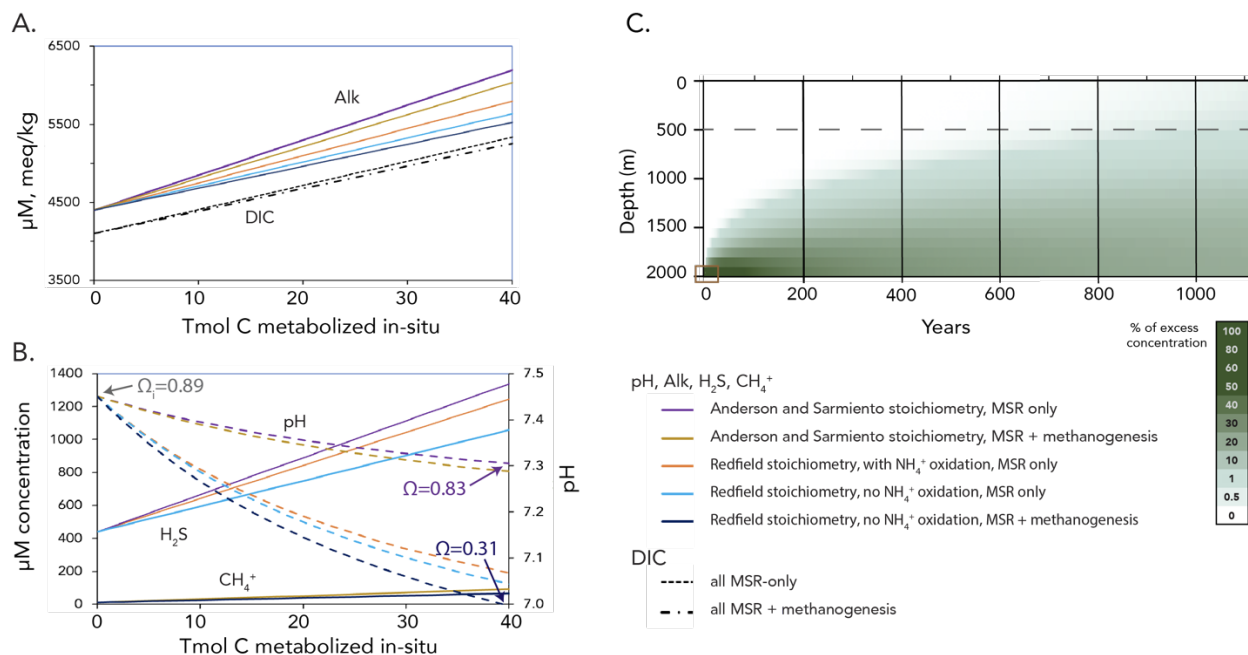
410 In Orca Basin, the primary control on transport from the basin to the upper water column is the strong  
411 density interface at 2220–2250 m depth. Durability of Orca Basin storage is assessed in the context of this  
412 mixing barrier rather than through a stacked diffusion model.

413

## 414 4. Results and Discussion

### 415 4.1 The Black Sea: Biogeochemical impacts of organic matter sequestration

416 We estimated the potential short-term (decadal) impacts of biomass addition to the deepest part of the  
417 western Black Sea using the scenarios defined in Table 1. To calculate the effects of mixing organic matter  
418 remineralization products into this environment, we use a volume of 32,398 km<sup>3</sup>, which is equivalent to  
419 ~43% of the total volume of the abyssal benthic boundary layer (75,137 km<sup>3</sup>). This reduced effective  
420 volume is an attempt to account for incomplete lateral mixing at depth and can be refined by future studies  
421 of advective flow dynamics within the layer (Markova, 2023). The amount of organic matter respired  
422 “instantaneously” *in situ* was varied from 0 to 40 Tmol C, which is equivalent to 0–1.76 Pg (Gt) CO<sub>2</sub>. Initial  
423 Black Sea deep water concentrations (NH<sub>3</sub> = 100 μM, H<sub>2</sub>S = 440 μM, TA = 4400 μM, DIC = 4100 μM)  
424 were taken from Hiscock and Millero (2006) and Dubinin et al. (2022). Salinity (22 psu) and temperature  
425 (8°C) were taken from Murray et al. (1991) (Fig. 2).



426

427 **Fig. 5 Impacts of enhanced organic matter breakdown in abyssal western Black Sea water. A –**  
 428 Calculated changes in DIC (dashed lines), and alkalinity concentrations (solid lines) resulting from the  
 429 instantaneous *in-situ* respiration of various total amounts of organic C by MSR (0 to 40 Tmol C), with or  
 430 without methanogenesis, for a range of organic matter stoichiometries (Table 1). In scenarios 4 and 5,  
 431 methanogenesis is presumed to metabolize 10% of respired organic C. **B** – Associated changes in abyssal  
 432 Black Sea sulfide and methane concentrations (solid lines) and pH (dashed lines) for various scenarios.  
 433 Annotations show the saturation state ( $\Omega$ ) of calcite (CaCO<sub>3</sub>), which is undersaturated throughout. **C** –  
 434 Modeled vertical mixing over time of a conservative tracer added to the Black Sea at >2,000 m depth. Water  
 435 depths above the dashed horizontal line experience advective flow.

436

437 If we consider only the effects of biomass respiration by MSR, ignoring methanogenic metabolisms and  
 438 subsequent reactions (e.g., sulfide oxidation; scenarios 1–3 in Table 1), we estimate that the microbial  
 439 respiration of 40 Tmol C below 2,000 m water depth would increase sulfide concentrations from a current  
 440 value of 440 µM to 1057–1337 µM, depending on mean organic C redox state (**Fig. 5**). Concurrently, in the  
 441 absence of ammonium oxidation, ammonium concentrations would increase from 100 µM to 279–296 µM;  
 442 these changes would be smaller for N-poor biomass. Because MSR generates alkalinity as well as CO<sub>2</sub>, the  
 443 pH change associated with this breakdown would be ~0.15 – 0.41 pH units. This is in notable contrast to  
 444 the oxic respiration of this same quantity of organic matter, which would cause pH to drop by more than 1  
 445 unit to a pH value of ~6.56 (calcite  $\Omega$  ~0.12) due to the absence of MSR-derived alkalinity. The deep Black

446 Sea is currently undersaturated with respect to calcite and aragonite, and therefore seafloor carbonates are  
 447 minor and unlikely to substantially buffer, or be substantially impacted by, changes in pH at this depth. At  
 448 even larger scales, the addition of 100 Tmol C (1.2 Pg C) respired via MSR *in situ* would raise deep-water  
 449 (>2,000 m) sulfide concentrations to nearly 2,000  $\mu\text{M}$  (from 400  $\mu\text{M}$ ) and drop pH to 6.87 (from 7.40).

	Mixing volume used	Example OC respired	Equivalent CO <sub>2</sub> stored	Area of 4-m-thick biomass (% of area)	Atm. comm. timescale
Black Sea	32,398 km <sup>3</sup>	40 Tmol C	3.5 to 11.7 Gt CO <sub>2</sub> e (50–85% efficiency)	2,160 – 7,219 km <sup>2</sup> (0.67–2.2% of area)	>1,000 yrs
Cariaco Basin	5,000 km <sup>3</sup>	2 Tmol C	0.18–0.59 Gt CO <sub>2</sub> e (50–85% efficiency)	111 – 364 km <sup>2</sup> (5.3–17% of west basin)	>10 yrs
Orca Basin	10.24 km <sup>3</sup>	0.05 Tmol C	0.005–0.26 Gt CO <sub>2</sub> e (50–98% efficiency)	3.1 – 158 km <sup>2</sup> (2 – 100% of brine area)	>10,000 yrs

450

451 **Table 2.** Scale of hypothetical scenarios discussed in the text. Equivalent CO<sub>2</sub> sequestration estimates apply  
 452 a wide range of storage “efficiency,” defined as the proportion of solid-phase biomass remaining unrespired  
 453 after ~decades. “Atm. comm. timescale” refers to the expected approximate lag between the production of  
 454 dissolved products and their potential communication to the surface ocean and atmosphere, discussed  
 455 below. We emphasize that these straw-man scenarios are intended as points of discussion and are not  
 456 prescriptive limits or goals for sequestration.

457 Biomass breakdown may also occur via methanogenic metabolisms. More experimental data is needed to  
 458 constrain the contribution of methanogenesis to biomass breakdown, which is likely to depend on biomass  
 459 type, the selected basin, and the engineered specifics of any proposed CDR operation (i.e., compression,  
 460 containment, and placement of biomass). Canonically, methanogenesis is repressed in the presence of  
 461 sulfate due to the slight energetic favorability of MSR (Froelich et al., 1979; Kristjansson et al., 1982). The  
 462 overall effect of MSR-driven breakdown on basin dissolved sulfate concentrations is small, but sulfate may  
 463 nonetheless be locally depleted, especially within interiors of sunken biomass or within underlying  
 464 sediments. Even when sulfate is present, however, methanogenic organisms are frequently capable of  
 465 operating alongside sulfate reducers using ‘non-competitive’ substrates like methanol or methylamine  
 466 (Oremland and Polcin, 1982; Zhuang et al., 2016); lignin methoxy groups can also fall into this category  
 467 (Hess et al., 2020). Additional data are needed to partition likely biomass breakdown for deep Black Sea  
 468 conditions into MSR and methanogenesis under a range of engineering conditions and placement scenarios.

469 We calculate the effects of methanogenesis on abyssal Black Sea geochemistry through Scenarios 4 and 5,  
 470 both of which make the assumption that 10% of total organic C breakdown moves through this pathway

471 and exclude the potential later reoxidation of methane. For the same scale of total C respiration discussed  
472 above (40 Tmol C), the addition of 2–2.9 Tmol CH<sub>4</sub> would increase abyssal methane concentrations from  
473 current values of ~10 uM to 71–100 uM and add the equivalent of roughly 10–15 yrs of natural CH<sub>4</sub>  
474 production in the shelf and slope sediments of the Black Sea (Reeburgh et al., 1991). Organic matter  
475 breakdown in these scenarios leads to slightly larger changes in abyssal pH and saturation state than MSR  
476 alone (Fig. 5) because methanogenesis does not produce alkalinity, unlike MSR. However, if the methane  
477 produced during methanogenesis is subsequently reoxidized anaerobically with sulfate, the summed  
478 reactions produce a net effect similar to breakdown via MSR alone (Middelburg et al., 2020).

479 One critical question impacting the feasibility of anoxic organic matter sequestration is the ability of local  
480 microbial communities to conduct anaerobic methane oxidation in the water column, removing methane  
481 from the system before it can escape to the atmosphere. Natural methane sources in the shelf and slope  
482 sediments of the Black Sea are large – approximately 0.29 Tmol CH<sub>4</sub>/yr (Reeburgh et al., 1991; Schmale  
483 et al., 2011) – and they are frequently local and episodic due to seafloor tectonic and other processes.  
484 Methane sinks balance these inputs, largely through methanotrophy (methane oxidation) in the anoxic water  
485 column of 1 to several hundred nM CH<sub>4</sub>/day and CH<sub>4</sub> fluxes into abyssal sediments (Reeburgh et al., 1991;  
486 Schmale et al., 2005). Studies in the similarly methane-rich Gulf of Mexico have observed 100-fold  
487 increases in methanotrophy rate constants in response to methane injection from the Deepwater Horizon oil  
488 spill (Kessler et al., 2011), and it has been argued that rates of Black Sea methanotrophy could respond  
489 similarly, given sufficient time for the methanotrophic community (with a doubling time of several months,  
490 Nauhaus et al., 2007) to grow (Schmale et al., 2011). Schmale et al. (2011) modeled the fate of the  
491 instantaneous injection of 11.2 Tmol CH<sub>4</sub> at 2,000 m water depth in the Black Sea (e.g., due to mid-depth  
492 hydrate destabilization or deep mud volcano eruptions) and concluded that this injection would cause a  
493 negligible 2–3% increase in the total modern Black Sea flux of methane to the atmosphere due to responsive  
494 rates of methanotrophy in the environment. Methanotrophy rates are also likely to show a positive  
495 relationship with increased methane concentrations as current methane concentrations in the Black Sea are  
496 near minimum thresholds for the activity of anaerobic methane oxidation (Valentine, 2011). Additional  
497 work is needed to validate these model results and better understand the capacity of these microbial methane  
498 oxidation processes to ‘scrub’ excess methane from the system.

499 Potential impacts of biogeochemical change in the abyssal Black Sea on human endeavors in the region are  
500 highly sensitive to the mixing, or lack thereof, between abyssal waters and the surface. The Black Sea is  
501 notably stratified, with minimal tidal action to add energy to the system (Stewart et al., 2007). We used  
502 estimates of eddy diffusivity (Ivanov and Samodurov, 2001) from water column profiles to calculate the  
503 rates at which dissolved products of organic C breakdown in the benthic boundary layer could be detected

504 near the shallow redoxcline (~150 m depth). As shown in Fig. 5, dissolved components added to deep water  
505 from biomass respiration can remain contained within >500 m-deep, slowly ventilating water masses over  
506 hundreds of years. As a percentage of the initial excess concentration in the deepest box, the excess  
507 concentration in the 500-m-deep water column box is approximately 0.04% after 400 yrs, 0.25% after 600  
508 yrs, 0.83% after 800 yrs, and 1.26% after 1,000 yrs. For a scenario with 40 Tg C addition and 600  $\mu\text{M}$  initial  
509 excess sulfide in the deepest box, this would be equivalent to an increase in the concentration of sulfide at  
510 500 m depth by 7.6  $\mu\text{M}$ , or roughly 5% of current concentrations, after 1,000 years. From the perspective  
511 of the upper, upwelling water column, impacts of dissolved species are within the range of natural  
512 variability (e.g. (Konovalov and Murray, 2001; Dubinin et al., 2022) for >1,000 years, assuming a roughly  
513 steady-state circulation in the Black Sea. Importantly, however, we do not yet fully understand the  
514 likelihood that stratification and ventilation rates in the Black Sea will substantially change in response to  
515 the changing hydrology and climate.

516 Although much of the energy from respiration of biomass is conserved in the short term, it will eventually  
517 contribute heat to the system that could impact deep vertical stratification of the water column. If we assume  
518 a rough energy yield of ~25 kJ/mol for MSR, the respiration of 40 Tmol C would generate  $\sim 10^{15}$  kJ, which,  
519 if released over very short timescale of ten years, could be a significant fraction of the natural geothermal  
520 heat flux driving convection in the benthic boundary layer of 0.04 W/m<sup>2</sup> (Zolotarev et al., 1979), or  $5.5 \cdot 10^{15}$   
521 kJ per decade. Changes in total energy flux and resulting water column stratification from metabolic  
522 processes could therefore become relevant for a hypothetical case of very large-scale, rapid implementation,  
523 but are otherwise unlikely to be significant.

524 All of the foregoing calculations focus solely on the products of *in situ* biomass respiration. Depending on  
525 the timescale being considered and the composition of sequestered biomass, respired C will represent some  
526 fraction of the total organic C added to the system. Initial experiments indicate that roughly 75% of lignin-  
527 rich terrestrial biomass may persist after 100 years of sedimentary storage under partially oxygenated  
528 conditions, and the efficiency of biomass storage is expected to be higher under anoxic conditions (Keil et  
529 al., 2010). For the purposes of this calculation, we apply a broad range of possible storage efficiencies  
530 between 50% and 85%, informed by these experiments and field observations. For this range of efficiencies,  
531 the in-situ respiration of 40 Tmol C discussed above translates into a total sequestration of 3.5 to 11.7 Pg  
532 (Gt) CO<sub>2</sub> equivalent. In such a hypothetical scenario, carbon would be stored in two distinct pools: 50-85%  
533 of sequestered carbon would be stored semi-permanently as solid biomass while 15–50% would be  
534 sequestered on a thousand-year timescale as either dissolved CO<sub>2</sub> or DOM. In terms of the physical size of  
535 such an installation, consolidated terrestrial biomass equivalent to 3.5 to 11.7 Pg CO<sub>2</sub> would, if deposited  
536 in a four-meter-thick layer in the deepest region of the western Black Sea, cover 2,160 – 7,219 km<sup>2</sup>, or

537 0.67–2.2% of total Black Sea area. The upper end of this range – a total amount, not an annual flux – is an  
538 enormous value, similar to the total production of crop waste across the entire planet in a year. Still, it  
539 represents only a third of a year of anthropogenic CO<sub>2</sub> emissions, underscoring the scale of the problem  
540 and the need for a broad portfolio of CDR techniques and rapid decarbonization to achieve global climate  
541 goals.

542 This highly simplified mass balance exercise suggests that the bulk geochemistry and stratification of the  
543 Black Sea may allow for moderate changes in the concentrations of H<sub>2</sub>S, NH<sub>4</sub>, alkalinity, and pH to result  
544 from the seafloor storage of a climatically relevant quantity of carbon. The scenario involving the in-situ  
545 respiration of ~40 Tmol C that we use for discussion purposes here (Table 2) is of the same order of  
546 magnitude in terms of increased organic C input as the 20<sup>th</sup>-century eutrophication of the Black Sea  
547 (Konovalov and Murray, 2001). Importantly, however, biomass breakdown in abyssal waters has a diluted  
548 and delayed effect on chemocline and mixed layer properties relative to shallow biomass breakdown.  
549 Geochemical changes within the basin are also isolated from the global ocean by the singular connection at  
550 the Bosphorus. This physical restriction provides spatial bounds for monitoring and verification of any CO<sub>2</sub>  
551 removal activities and isolates its impacts to a relatively well-defined set of stakeholders in the region.

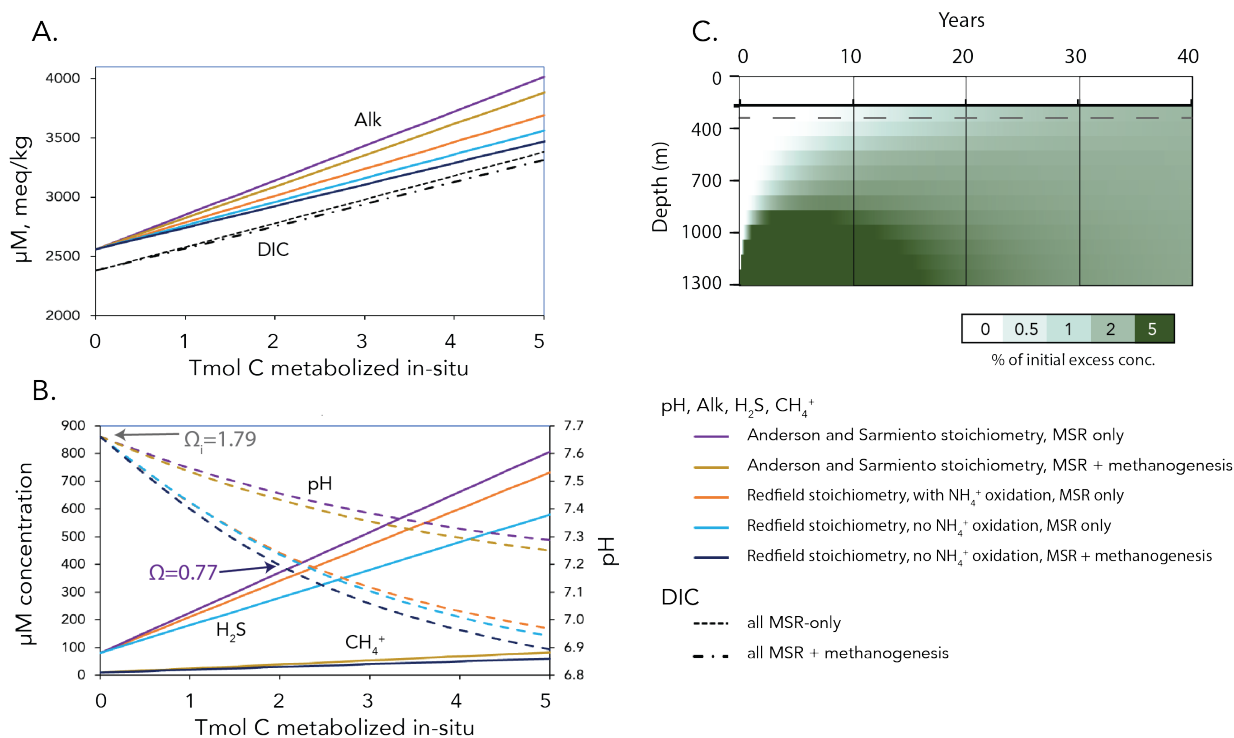
552 Despite the potential for gigatonne-scale CO<sub>2</sub> sequestration suggested by these broad calculations, we  
553 emphasize that this preliminary analysis has many limitations and also identifies potential risks that will  
554 require additional research. We assume that remineralization products mix rapidly within a volume  
555 equivalent to slightly less than half of the entire deep benthic boundary layer, neglecting acute or local  
556 impacts, which may be especially important for predicting sedimentary methane production. We do not  
557 explicitly consider reactions that re-oxidize sulfide or methane, and we do not yet have the experimental  
558 data to support precise predictions of biomass consumption via methanogenesis or methane reoxidation via  
559 methanotrophy. We also lack the necessary data to evaluate how seafloor heterotrophic communities –  
560 bacteria, archaea, and potentially fungi – will respond to a massive influx of biomass in this environment.  
561 And finally, more data is needed to constrain physical mixing and circulation within the deep Black Sea  
562 benthic boundary layer. It is our aim that these results motivate rigorous field and experimental studies to  
563 develop more nuanced models for the durability and ecological impacts of biomass storage in the Black  
564 Sea.

565

#### 566 **4.2 Cariaco Basin: Biogeochemical impacts of organic carbon sequestration**

567 Using the same general approach and stoichiometric scenarios (Table 1) that we used for the Black Sea, we  
568 estimated the potential effects of biomass addition to the deep seafloor of Cariaco Basin. The amount of

569 organic matter respired in situ was varied from 0 to 5 Tmol C, and initial geochemical conditions for the  
 570 deep Basin are summarized in Figure 2.



571  
 572 **Figure 6. Effects of enhanced OM breakdown on Cariaco Basin water chemistry** below 350 m water  
 573 depth, based on scenarios in Table 1. In scenarios 4 and 5, methanogenesis is presumed to metabolize 10%  
 574 of total respired organic C. **A** – Concentrations of DIC (dashed) and alkalinity (solids) following various  
 575 scenarios for the instantaneous addition and respiration of various quantities of biomass. **B** – Concentrations  
 576 of sulfide or methane (solid lines) and pH (dashed) following various scenarios; sulfide concentrations in  
 577 MSR-only scenarios 1 and 4 are the same for mixed-metabolism scenarios 2 and 5, respectively.  
 578 Annotations show the saturation state ( $\Omega$ ) of calcite ( $\text{CaCO}_3$ ) for 0 and 2 Tg C. **C** – Mixing of a conservative  
 579 tracer in the western Cariaco Basin over several decades. Calculations conservatively use eddy diffusion  
 580 coefficients from Scranton (1987), although these lead to  $\sim 10\times$  faster mixing than the values assumed by  
 581 earlier work (Fanning and Pilson, 1972; Reeburgh, 1976).

582  
 583 The vertical circulation and mixing timescale of Cariaco Basin are very different from the case of the Black  
 584 Sea. Cariaco Basin is relatively well mixed below the chemocline at 350 m depth but is divided into eastern  
 585 and western sub-basins that lack lateral mixing. Given seasonal upwelling and weak stratification in the  
 586 basin, dissolved species from the deepest part of the basin reach the chemocline depth within about 20 years

587 (Fig. 6). Accordingly, to assess the geochemical impacts of CDR-scale biomass addition, we calculated  
588 potential changes in deep water chemistry for this full volume of  $\sim 5,000 \text{ km}^3$ . The remineralization of 2  
589 Tmol of organic C in this volume (Table 2) increases modeled sulfide concentrations from an initial value  
590 of 80  $\mu\text{M}$  to 262–375  $\mu\text{M}$ , depending on the stoichiometry of the organic matter source and the metabolic  
591 pathways used (scenarios 1–5). This amount of remineralization would also cause increases in  $\text{NH}_4^+$  (from  
592 20  $\mu\text{M}$  to 75–82  $\mu\text{M}$ ) and  $\text{CH}_4$  (from 10  $\mu\text{M}$  to 28–36  $\mu\text{M}$ ). The appearance of excess sulfide and ammonium  
593 at the chemocline will enhance  $\text{O}_2$  demand and may shoal the water column oxic-anoxic interface. More  
594 complex modeling efforts will be required to assess these dynamic interactions and the many linked redox  
595 reactions they impact near the chemocline.

596 The pH change associated with the in situ remineralization of 2 Tmol of relatively reduced (lipid-rich)  
597 organic carbon (scenarios 1 and 4) is  $\sim 0.2$  units (from 7.66 to 7.45), while the pH change for more oxidized  
598 organic carbon (scenarios 2, 3, and 5) is 0.43 units (from 7.66 to 7.23). Unlike the Black Sea, the deep  
599 Cariaco Basin is supersaturated with respect to  $\text{CaCO}_3$  (calcite  $\Omega = 1.79$ ). The larger pH change associated  
600 with scenarios 2, 3, and 5 would drive calcite to be undersaturated ( $\Omega = 0.77$ ), favoring dissolution (Fig.  
601 6). Actual pH change would be strongly buffered by reactions with highly abundant carbonates in Cariaco  
602 Basin sediments (Aguilar et al., 2017), which would add alkalinity to deep water.

603 The effectiveness of Cariaco Basin as a site for biomass storage and CDR is far more sensitive to the  
604 efficiency of biomass breakdown than the Black Sea because its weak density gradient and history of  
605 dynamic redox change raise the possibility of deep mixing and ventilation. Key targets for future research  
606 include this biomass breakdown efficiency and its trajectory over time, as well as understanding the  
607 responsiveness of water column methane oxidizing organisms to changes in methane flux. Using a range  
608 of estimates for terrestrial biomass storage efficiencies over several decades of 50–85% (Keil et al., 2010),  
609 the in-situ respiration of 2 Tmol C could represent a total initial carbon sequestration of 0.18–0.59 Pg  $\text{CO}_2$   
610 equivalents, with part stored as solid-phase bales stable over centennial timescales and the remainder  
611 present dissolved species with lower durability. In this scenario, this quantity of baled biomass in a 4-meter-  
612 thick layer would physically cover 5.3–17% of the western sub-basin seafloor ( $>1000 \text{ m}$  depth,  $2100 \text{ km}^2$   
613 area, Scranton, 1988). Establishing acceptable limits for environmental change requires collaboration by  
614 many stakeholders, most critically the local Venezuelan communities that are economically invested in  
615 both fisheries and any future CDR industry. As a first-order evaluation to guide this multi-stakeholder  
616 decision making, however, Cariaco Basin appears to have sufficient biogeochemical capacity to support  
617 meaningful quantities of biomass carbon storage and is deserving of further research attention, most  
618 importantly to address uncertainties related to upwelling and storage durability.

619

### 620 4.3 Orca Basin and other hypersaline basins

621 Orca Basin is much smaller than either the Black Sea or Cariaco Basin, with a total brine volume of just  
622  $10.2 \text{ km}^3$  (compared to  $5,000 \text{ km}^3$  for Cariaco or  $32,398 \text{ km}^3$  for the Black Sea). We can assess some aspects  
623 of the response of Orca Basin to the placement and remineralization of organic matter, but the extreme ionic  
624 strength of Orca Basin exceeds the range of known equilibrium constants for the carbonate system and  
625 prevents meaningful pH calculations. We also lack sufficient understanding of the unusual Orca Basin  
626 microbial community (Nigro et al., 2020) to constrain the relative importance of methanogenesis and MSR  
627 within the brine, adding uncertainty to model results (Table 2). For illustration purposes, however, we can  
628 assume that some fraction of sequestered biomass breaks down through MSR and/or methanogenesis at a  
629 rate that is at least much faster than the rate of mixing across the water-brine interface.

630 The microbial community in Orca Basin consists primarily of halophilic sulfate reducers, methanogens,  
631 and ammonium oxidizers (Nigro et al., 2020), and rates of potential sulfate reduction are low, similar to  
632 other hypersaline brines ( $\sim 10$  to  $76 \text{ nmol cm}^{-3} \text{ d}^{-1}$ ; Hurtgen et al., 1999; Zhuang et al., 2016). Despite low  
633 rates of MSR and methanogenesis, Orca Basin is highly effective at preserving of at least some types of  
634 organic matter. Well-preserved seaweeds and their epibionts and lipids have been described from Orca  
635 Basin sediments below 10 m depth, which is virtually unheard of in other settings (Kennett and Penrose,  
636 1978; Harvey and Kennicutt, 1992) and indicates a remarkable absence or selectivity of heterotrophic  
637 degradation. Although electron acceptors (e.g., sulfate) are plentiful, organic materials are also abundant  
638 within the brine: DOM concentrations reach  $0.24 \text{ mM DOC}$ , and sinking particulate organic matter provides  
639 a consistent marine C source (Trefry, 1984; Shah et al., 2013; Diercks et al., 2019). We can therefore  
640 constrain the maximum rates of biomass breakdown in Orca Basin from field observations and sediment  
641 core data, while the minimum rates of breakdown for some biomass types may approach zero. We explore  
642 relevant sequestration scales using an extremely conservative value of 50% for the minimum biomass  
643 retention efficiency and a maximum efficiency of 98%, which is based on observations of extremely slow  
644 biomass breakdown and intact Sargassum materials in the sediments.

645 Given the small volume of the brine, the *in situ* respiration of  $0.05 \text{ Tmol C}$  ( $2.2 \text{ Tg CO}_2$  equivalent) by only  
646 MSR (no methanogenesis) would increase DIC concentrations from  $4.7 \text{ mM}$  to  $9.6 \text{ mM}$  and simultaneously  
647 increase alkalinity from  $4.4 \text{ mM}$  to between  $9.3$  and  $11.4 \text{ mM}$ , depending on mean respired organic matter  
648 redox state. This amount of MSR would generate  $2.4\text{--}3.5 \text{ mM H}_2\text{S}$ , much of which would likely be removed  
649 by subsequent reactions with iron to form iron sulfide minerals (Van Cappellen et al., 1998). Redfieldian  
650 biomass would increase  $\text{NH}_4^+$  from  $0.5 \text{ mM}$  to  $\sim 1.2 \text{ mM}$ , although changes would be smaller for high C:N  
651 materials. Alternatively, if 10% of breakdown proceeded via (methylotrophic) methanogenesis, breakdown  
652 of the same amount of organic carbon could increase DIC from  $4.7 \text{ mM}$  to  $6.1\text{--}9.6 \text{ mM}$  without adding

653 alkalinity, lowering brine pH. The resulting methane would be sufficient to increase the already high natural  
654 concentrations of CH<sub>4</sub> in the brine (to 1.1 mM from 0.75 mM). Regardless of breakdown pathway, 0.05  
655 Tmol C may translate into meaningful quantities of CO<sub>2</sub> storage, but this calculation is highly sensitive to  
656 actual breakdown rates for the biomass type chosen. A 4-meter-thick layer of biomass across the entire  
657 deep Orca Basin brine region (158 km<sup>2</sup>, Diercks et al., 2019) could contain as much as 0.26 Pg CO<sub>2</sub>e and  
658 would release ~0.05 Tmol C if it were 98% efficient. As for the other case studies, this calculation assumes  
659 highly idealized engineering scenarios and considers only immediate geochemical breakdown products  
660 without time-resolved processes. Extensive further analytical and modeling work are needed to evaluate  
661 the downstream impacts of geochemical change within the Basin and to understand their interactions with  
662 microbial ecology, DOM, and mixing across the pycnocline.

663 A critical knowledge gap for evaluating Orca Basin CO<sub>2</sub> removal potential is the how its slow-growing  
664 microbial community would respond to a dramatic increase in carbon availability. Experiments are also  
665 needed to assess the relative importance of sulfate reduction versus methylotrophic methanogenesis for  
666 biomass breakdown in hypersaline basins, the rates of these processes, and the sensitivity of breakdown  
667 rates to hypersaline conditions. Evidence for stimulated methanogenesis could represent a risk for enhanced  
668 methane release to the overlying water column, and although oxic methanotrophy in the Gulf of Mexico  
669 can be relatively efficient (Kessler et al., 2011), the response of aerobic methane oxidizers in the water  
670 column requires further investigation.

671 Due to minimal mixing across the pycnocline, both solid- and dissolved-phase C in this system would be  
672 physically sequestered over thousand-year timescales. The effects of stimulated MSR are likely limited to  
673 the brine itself, although significant sulfide addition would make the brine sulfidic and impact metal  
674 cycling, primarily that of Fe and Mn. In order to assess the release of breakdown products and background  
675 hydrocarbons to the overlying water column in either endmember case, field data are needed related to how  
676 biomass sinking impacts mixing at the Orca Basin pycnocline. The scale of potential mixing in a real  
677 deployment would depend on the engineering choices that allow ballasted or densified biomass to sink  
678 through the pycnocline.

679

## 680 **5. Summary and Conclusions: CDR potential of anoxic basins and key unknowns**

681 Any future attempts at effective and responsible CDR are futile in the absence of immediate and dramatic  
682 CO<sub>2</sub> emissions reductions on a global scale and must be pursued in that context; emissions reductions are  
683 the most cost-effective and highest net reduction strategy currently available (IPCC AR6, 2023). If marine  
684 CDR is pursued as an approach to support decarbonization, its methods will need to both minimize

685 ecological risks and maximize storage durability. Risk minimization will also require effective monitoring,  
686 reporting, and verification (MRV) to account for the actual efficiency and durability of CO<sub>2</sub> storage in  
687 various parts of the ocean system.

688 By these criteria, anoxic basins in general and the Black Sea in particular may represent uniquely effective  
689 locations for the durable sequestration of atmospheric CO<sub>2</sub> as organic carbon, conceptually accelerating a  
690 central mechanism for climate recovery in the natural Earth system. Although anoxia can also be present in  
691 environments like fjords, river deltas, lakes, and upwelling zones, these systems are generally more  
692 challenging for CO<sub>2</sub> sequestration because they lack the scale, stability, sulfate availability, and/or isolation  
693 of permanently anoxic marine basins. Anoxic basins may reduce geochemical and ecological risks relative  
694 to well-oxygenated regions, where biomass degradation will have larger impacts on pH, deoxygenation,  
695 and deep-sea ecosystems (Levin et al., 2023). These regions also avoid risks of carbon mobilization due to  
696 bottom trawling or seabed mining, and they minimize the economic, social, and political complexities of  
697 work in coastal environments. Nonetheless, deep-sea microbial ecosystems have substantial value for  
698 microbial diversity, exobiology research, and the preservation of sedimentary records, along with  
699 opportunities for future discovery. All of these factors will need to be balanced against potential marginal  
700 reductions in harmful climate outcomes when making future decisions about trial or full-scale deployments  
701 of biomass-based marine CDR. Future decision making must also consider the full life-cycle of biomass  
702 sources, which are excluded from analysis here.

703 The effective capacity of anoxic basins for CO<sub>2</sub> removal depends on both the efficiency of organic carbon  
704 storage, which depends in turn on the stoichiometry and reactivity of the biomass materials selected, and  
705 its durability, which is also a function of site circulation. Although the Black Sea has by far the largest  
706 capacity for organic carbon sequestration, smaller but complementary contributions may be achievable  
707 from Cariaco Basin and anoxic hypersaline basins like Orca Basin. A primary challenge for CDR  
708 applications in Cariaco Basin will be the high and variable rates of upwelling in the basin, which will  
709 ventilate remineralized CO<sub>2</sub>. For Orca Basin, a primary challenge is predicting biogeochemical behavior in  
710 brines with unusual chemistry, necessitating site-specific studies of the relative favorability of microbial  
711 breakdown processes. In all of these cases, the often restricted circulation of anoxic marine basins presents  
712 opportunities for effective monitoring, reporting and verification of CO<sub>2</sub> sequestration and environmental  
713 effects. The combination of pH, DIC, and alkalinity data can constrain the relative rates of organic matter  
714 remineralization via microbial sulfate reduction and methanogenesis.

715 If future work concludes that the biomass storage efficiency in the Black Sea and Orca Basin is high on  
716 relevant timescales (e.g., 85% over decades or more) and that benefits of action outweigh risks, then  
717 biomass storage at these sites might be able to contribute to global CDR goals of 1–10 Pg CO<sub>2</sub>e/yr (2.5 –

718 25% of current annual emissions). For the hypothetical scenarios in Table 2, the Black Sea and Orca Basin  
719 might together sequester on the order of 10 Pg CO<sub>2</sub>e total, or about a year of humanity's CDR needs over  
720 the next century (IPCC AR6, 2021). An enormous effort will be required to develop a suite of parallel CDR  
721 approaches that can achieve ongoing CO<sub>2</sub> storage at the required scale.

722 Additional research is needed to fill several key gaps in our ability to predict carbon cycling impacts of  
723 organic matter addition to anoxic basins and to inform decision making related to its potential future  
724 implementation as a CDR strategy. At a minimum, we will need to (1) test and parameterize  
725 remineralization rates for specific types and components of biomass under relevant conditions, including  
726 within the interiors of biomass installations; (2) investigate the scale and recalcitrance of DOM generated  
727 from sequestered biomass; (3) evaluate the impacts of biomass placement on benthic carbon turnover and  
728 chemical profiles in sediments, and (4) develop basin-specific models for the physical transport and mixing  
729 effects of potential operations. The remaining scientific challenges are substantial, but anoxic marine basins  
730 have the potential to be substantive contributors to a global portfolio of CO<sub>2</sub> removal technologies and  
731 should be a priority for additional focused investigation.

732

733

#### 734 **Open Research**

735 No data or software were produced as part of this study.

736

#### 737 **Acknowledgments**

738 We thank Adam Subhas (WHOI) and Max Lloyd (Penn State) for valuable discussions about carbonate  
739 chemistry and lignin breakdown pathways. We also thank Cameron Allen (UCSB) for his assistance with  
740 the early stages of the project. Funding for this work was provided by a grant to UCSB from the  
741 Grantham Foundation for the Protection of the Environment.

742

#### 743 **Conflict of Interest Statement**

744 In addition to her primary role as UCSB faculty, Raven serves as the Chief Science Officer for, and holds  
745 equity in, Carboniferous, Inc., a seed-funded startup company exploring potential applications of deep  
746 marine biomass sequestration. The research presented here was conducted and funded entirely via research  
747 grants to UCSB. An unconflicted PI is formally involved for all CDR-related funds and mentorship plans  
748 in the Raven group. No other co-authors have real or perceived COIs to disclose.

749

750

751

752 **References**

753

754 Addy S. K. and Behrens E. W. (1980) Time of accumulation of hypersaline anoxic brine in Orca  
755 basin (Gulf of Mexico). *Marine Geology* **37**, 241–252.

756 Aguilar I., Sabatier P., Beck C., Audemard F., Crouzet C., Urbani F. and Campos C. (2017)  
757 Calculation of the reservoir age from organic and carbonate fractions of sediments in  
758 the Gulf of Cariaco (Caribbean Sea). *Quaternary Geochronology* **38**, 50–60.

759 Aller R. C. (1994) Bioturbation and remineralization of sedimentary organic matter: effects of  
760 redox oscillation. *Chemical Geology*, 15.

761 Aller R. C. and Cochran J. K. (2019) The Critical Role of Bioturbation for Particle Dynamics,  
762 Priming Potential, and Organic C Remineralization in Marine Sediments: Local and Basin  
763 Scales. *Front. Earth Sci.* **7**, 157.

764 Anderson L. A. and Sarmiento J. L. (1994) Redfield ratios of remineralization determined by  
765 nutrient data analysis. *Global Biogeochem. Cycles* **8**, 65–80.

766 Armstrong McKay D. I., Staal A., Abrams J. F., Winkelmann R., Sakschewski B., Loriani S., Fetzer  
767 I., Cornell S. E., Rockström J. and Lenton T. M. (2022) Exceeding 1.5°C global warming  
768 could trigger multiple climate tipping points. *Science* **377**, eabn7950.

769 Ballard R. D., Hiebert F. T., Coleman D. F., Ward C., Smith J. S., Willis K., Foley B., Croff K., Major  
770 C. and Torre F. (2001) Deepwater Archaeology of the Black Sea: The 2000 Season at  
771 Sinop, Turkey. *American Journal of Archaeology* **105**, 607–623.

772 Bambach R. K. (2006) Phanerozoic Biodiversity Mass Extinctions. *Annu. Rev. Earth Planet. Sci.*  
773 **34**, 127–155.

774 Benner R., Maccubbin A. E. and Hodson R. E. (1984) Anaerobic Biodegradation of the Lignin and  
775 Polysaccharide Components of Lignocellulose and Synthetic Lignin by Sediment  
776 Microflora. *Appl Environ Microbiol* **47**, 998–1004.

777 Benner R., Moran M. A. and Hodson R. E. (1986) Biogeochemical cycling of lignocellulosic  
778 carbon in marine and freshwater ecosystems: Relative contributions of procaryotes and  
779 eucaryotes1: Aquatic lignocellulose degradation. *Limnol. Oceanogr.* **31**, 89–100.

780 Bianchi T. S., Cui X., Blair N. E., Burdige D. J., Eglinton T. I. and Galy V. (2018) Centers of organic  
781 carbon burial and oxidation at the land-ocean interface. *Organic Geochemistry* **115**,  
782 138–155.

- 783 Boyd P. W., Bach L. T., Hurd C. L., Paine E., Raven J. A. and Tamsitt V. (2022) Potential negative  
784 effects of ocean afforestation on offshore ecosystems. *Nat Ecol Evol* **6**, 675–683.
- 785 Boye K., Noël V., Tfaily M. M., Bone S. E., Williams K. H., Bargar J. R. and Fendorf S. (2017)  
786 Thermodynamically controlled preservation of organic carbon in floodplains. *Nature*  
787 *Geosci* **10**, 415–419.
- 788 Committee on A Research Strategy for Ocean-based Carbon Dioxide Removal and  
789 Sequestration, Ocean Studies Board, Division on Earth and Life Studies, and National  
790 Academies of Sciences, Engineering, and Medicine (2022) *A Research Strategy for*  
791 *Ocean-based Carbon Dioxide Removal and Sequestration.*, National Academies Press,  
792 Washington, D.C.
- 793 Cowie G. L. and Hedges J. I. (1992) Sources and reactivities of amino acids in a coastal marine  
794 environment. *Limnol. Oceanogr.* **37**, 703–724.
- 795 Diercks A., Ziervogel K., Sibert R., Joye S. B., Asper V. and Montoya J. P. (2019) Vertical marine  
796 snow distribution in the stratified, hypersaline, and anoxic Orca Basin (Gulf of Mexico)  
797 eds. J. W. Deming and L. Thomsen. *Elementa: Science of the Anthropocene* **7**, 10.
- 798 van Dongen B. E., Schouten S. and Sinninghe Damsté J. S. (2006) Preservation of carbohydrates  
799 through sulfurization in a Jurassic euxinic shelf sea: Examination of the Blackstone Band  
800 TOC cycle in the Kimmeridge Clay Formation, UK. *Organic Geochemistry* **37**, 1052–1073.
- 801 Du Vivier A. D. C., Jacobson A. D., Lehn G. O., Selby D., Hurtgen M. T. and Sageman B. B. (2015)  
802 Ca isotope stratigraphy across the Cenomanian–Turonian OAE 2: Links between  
803 volcanism, seawater geochemistry, and the carbonate fractionation factor. *Earth and*  
804 *Planetary Science Letters* **416**, 121–131.
- 805 Dubinin A. V., Demidova T. P., Dubinina E. O., Rimskaya-Korsakova M. N., Semilova L. S.,  
806 Berezhnaya E. D., Klyuvitkin A. A., Kravchishina M. D. and Belyaev N. A. (2022) Sinking  
807 particles in the Black Sea waters: Vertical fluxes of elements and pyrite to the bottom,  
808 isotopic composition of pyrite sulfur, and hydrogen sulfide production. *Chemical*  
809 *Geology* **606**, 120996.
- 810 Egorov V. N., Artemov Y. G., Gulin S. B. and Polikarpov G. (2011) Methane seeps in the Black  
811 Sea: discovery, quantification and environmental assessment. , 15.
- 812 Fanning K. A. and Pilson M. E. Q. (1972) A model for the anoxic zone of the Cariaco Trench.  
813 *Deep Sea Research and Oceanographic Abstracts* **19**, 847–863.
- 814 Fenchel T. (2012) Protozoa and oxygen. *Acta protozoologica* **52**, 11.
- 815 Fraser C. I., Nikula R. and Waters J. M. (2011) Oceanic rafting by a coastal community. *Proc. R.*  
816 *Soc. B.* **278**, 649–655.

- 817 Froelich P. N., Klinkhammer G. P., Bender M. L., Luedtke N. A., Heath G. R., Cullen D., Dauphin P.  
 818 and Blaynehartman D. Hammond. (1979) Early oxidation of organic matter in pelagic  
 819 sediments of the eastern equatorial Atlantic: suboxic diagenesis. *Geochimica et*  
 820 *Cosmochimica Acta* **43**, 1075–1090.
- 821 Gallagher K. L., Kading T. J., Braissant O., Dupraz C. and Visscher P. T. (2012) Inside the alkalinity  
 822 engine: the role of electron donors in the organomineralization potential of sulfate-  
 823 reducing bacteria. *Geobiology* **10**, 518–530.
- 824 Hartnett H. E., Keil R. G., Hedges J. I. and Devol A. H. (1998) Influence of oxygen exposure time  
 825 on organic carbon preservation in continental margin sediments. *Nature* **391**, 572–575.
- 826 Harvey H. R. and Kennicutt M. C. (1992) Selective alteration of Sargassum lipids in anoxic  
 827 sediments of the Orca Basin. *Organic Geochemistry* **18**, 181–187.
- 828 Hastings D. and Emerson S. (1988) Sulfate reduction in the presence of low oxygen levels in the  
 829 water column of the Cariaco Trench: Oxidative sulfate reduction. *Limnol. Oceanogr.* **33**, 391–  
 830 396.
- 831 Hedges J. I. and Keil R. G. (1995) Sedimentary organic matter preservation: an assessment and  
 832 speculative synthesis. *Marine Chemistry* **49**, 81–115.
- 833 Hess M., Paul S. S., Puniya A. K., van der Giezen M., Shaw C., Edwards J. E. and Fliegerová K.  
 834 (2020) Anaerobic Fungi: Past, Present, and Future. *Front. Microbiol.* **11**, 584893.
- 835 Hiscock W. T. and Millero F. J. (2006) Alkalinity of the anoxic waters in the Western Black Sea.  
 836 *Deep Sea Research Part II: Topical Studies in Oceanography* **53**, 1787–1801.
- 837 Hülse D., Arndt S. and Ridgwell A. (2019) Mitigation of Extreme Ocean Anoxic Event Conditions  
 838 by Organic Matter Sulfurization. *Paleoceanography and Paleoclimatology* **34**, 476–489.
- 839 Hülse D., Lau K. V., van de Velde S. J., Arndt S., Meyer K. M. and Ridgwell A. (2021) End-Permian  
 840 marine extinction due to temperature-driven nutrient recycling and euxinia. *Nat. Geosci.*  
 841 **14**, 862–867.
- 842 Hulthe G., Hulth S. and Hall P. O. J. (1998) Effect of oxygen on degradation rate of refractory  
 843 and labile organic matter in continental margin sediments. *Geochimica et Cosmochimica*  
 844 *Acta* **62**, 1319–1328.
- 845 Hurtgen M. T., Lyons T., Ingall E. and Cruse A. (1999) Anomalous enrichments of iron  
 846 monosulfide in euxinic marine sediments and the role of H<sub>2</sub>S in iron sulfide  
 847 transformations; examples from Effingham Inlet, Orca Basin, and the Black Sea.  
 848 *American Journal of Science* **299**, 556–588.
- 849 Ivanov L. I. and Samodurov A. S. (2001) The role of lateral fluxes in ventilation of the Black Sea.  
 850 *Journal of Marine Systems* **31**, 159–174.

- 851 Jarvis I., Lignum J. S., Gröcke D. R., Jenkyns H. C. and Pearce M. A. (2011) Black shale deposition,  
 852 atmospheric CO<sub>2</sub> drawdown, and cooling during the Cenomanian-Turonian Oceanic  
 853 Anoxic Event: CO<sub>2</sub> drawdown and cooling during OAE2. *Paleoceanography* **26**, n/a-n/a.
- 854 Jørgensen B. B., Weber A. and Zopfi J. (2001) Sulfate reduction and anaerobic methane  
 855 oxidation in Black Sea sediments. *Deep Sea Research Part I: Oceanographic Research*  
 856 *Papers* **48**, 2097–2120.
- 857 Keil R. G., Nuwer J. M. and Strand S. E. (2010) Burial of agricultural byproducts in the deep sea  
 858 as a form of carbon sequestration: A preliminary experiment. *Marine Chemistry* **122**,  
 859 91–95.
- 860 Kennett J. P. and Penrose N. L. (1978) Fossil Holocene seaweed and attached calcareous  
 861 polychaetes in an anoxic basin, Gulf of Mexico. *Nature* **276**, 172–173.
- 862 Kessler J. D., Valentine D. L., Redmond M. C., Du M., Chan E. W., Mendes S. D., Quiroz E. W.,  
 863 Villanueva C. J., Shusta S. S., Werra L. M., Yvon-Lewis S. A. and Weber T. C. (2011) A  
 864 Persistent Oxygen Anomaly Reveals the Fate of Spilled Methane in the Deep Gulf of  
 865 Mexico. *Science* **331**, 312–315.
- 866 Kohnen M. E. L., Damsté J. S. S., Kock-van Dalen A. C., Haven H. L. T., Rullkötter J. and De Leeuw  
 867 J. W. (1990) Origin and diagenetic transformations of C<sub>25</sub> and C<sub>30</sub> highly branched  
 868 isoprenoid sulphur compounds: Further evidence for the formation of organically bound  
 869 sulphur during early diagenesis. *Geochimica et Cosmochimica Acta* **54**, 3053–3063.
- 870 Konovalov S. K. and Murray J. W. (2001) Variations in the chemistry of the Black Sea on a time  
 871 scale of decades (1960–1995). *Journal of Marine Systems* **31**, 217–243.
- 872 Krause-Jensen D. and Duarte C. M. (2016) Substantial role of macroalgae in marine carbon  
 873 sequestration. *Nature Geosci* **9**, 737–742.
- 874 Kristjansson J. K., Schønheit P. and Thauer R. K. (1982) Different K<sub>s</sub> values for hydrogen of  
 875 methanogenic bacteria and sulfate reducing bacteria: An explanation for the apparent  
 876 inhibition of methanogenesis by sulfate. *Arch. Microbiol.* **131**, 278–282.
- 877 Kuhnt W., Holbourn A. E., Beil S., Aquit M., Krawczyk T., Flögel S., Chellai E. H. and Jabour H.  
 878 (2017) Unraveling the onset of Cretaceous Oceanic Anoxic Event 2 in an extended  
 879 sediment archive from the Tarfaya-Laayoune Basin, Morocco: Tarfaya OAE2 Onset.  
 880 *Paleoceanography* **32**, 923–946.
- 881 LaRock P. A., Lauer R. D., Schwarz J. R., Watanabe K. K. and Wiesenburg D. A. (1979) Microbial  
 882 Biomass and Activity Distribution in an Anoxic, Hypersaline Basin. *Appl Environ Microbiol*  
 883 **37**, 466–470.

- 884 Lee B.-S., Bullister J. L., Murray J. W. and Sonnerup R. E. (2002) Anthropogenic  
 885 chlorofluorocarbons in the Black Sea and the Sea of Marmara. *Deep Sea Research Part I:*  
 886 *Oceanographic Research Papers* **49**, 895–913.
- 887 Lee C. (1992) Controls on organic carbon preservation: The use of stratified water bodies to  
 888 compare intrinsic rates of decomposition in oxic and anoxic systems. *Geochimica et*  
 889 *Cosmochimica Acta* **56**, 3323–3335.
- 890 Levin L. A., Alfaro-Lucas J. M., Colaço A., Cordes E. E., Craik N., Danovaro R., Hoving H.-J., Ingels  
 891 J., Mestre N. C., Seabrook S., Thurber A. R., Vivian C. and Yasuhara M. (2023) Deep-sea  
 892 impacts of climate interventions. *Science* **379**, 978–981.
- 893 Li M., Pu Y. and Ragauskas A. J. (2016) Current Understanding of the Correlation of Lignin  
 894 Structure with Biomass Recalcitrance. *Front. Chem.* **4**.
- 895 Lyons W. B., Long D. T., Hines M. E., Gaudette H. E. and Armstrong P. B. (1984) Calcification of  
 896 cyanobacterial mats in Solar Lake, Sinai. *Geol* **12**, 623.
- 897 Marchand C., Disnar J. R., Lallier-Vergès E. and Lottier N. (2005) Early diagenesis of  
 898 carbohydrates and lignin in mangrove sediments subject to variable redox conditions  
 899 (French Guiana). *Geochimica et Cosmochimica Acta* **69**, 131–142.
- 900 Markova N. V. (2023) The Black Sea Deep-Water Circulation: Recent Findings and Prospects for  
 901 Research. In *Processes in GeoMedia—Volume VI* (ed. T. Chaplina). Springer Geology.  
 902 Springer International Publishing, Cham. pp. 553–564.
- 903 Mayumi D., Mochimaru H., Tamaki H., Yamamoto K., Yoshioka H., Suzuki Y., Kamagata Y. and  
 904 Sakata S. (2016) Methane production from coal by a single methanogen. *Science* **354**,  
 905 222–225.
- 906 Middelburg J. J., Soetaert K. and Hagens M. (2020) Ocean Alkalinity, Buffering and  
 907 Biogeochemical Processes. *Rev. Geophys.* **58**.
- 908 Muller-Karger F. E., Astor Y. M., Benitez-Nelson C. R., Buck K. N., Fanning K. A., Lorenzoni L.,  
 909 Montes E., Rueda-Roa D. T., Scranton M. I., Tappa E., Taylor G. T., Thunell R. C., Troccoli  
 910 L. and Varela R. (2019) The Scientific Legacy of the CARIACO Ocean Time-Series  
 911 Program. *Annu. Rev. Mar. Sci.* **11**, 413–437.
- 912 Muller-Karger F., Varela R., Thunell R., Astor Y., Zhang H., Luerssen R. and Hu C. (2004)  
 913 Processes of coastal upwelling and carbon flux in the Cariaco Basin. *Deep Sea Research*  
 914 *Part II: Topical Studies in Oceanography* **51**, 927–943.
- 915 Murray J. W., Top Z. and Özsoy E. (1991) Hydrographic properties and ventilation of the Black  
 916 Sea. *Deep Sea Research Part A. Oceanographic Research Papers* **38**, S663–S689.

- 917 Nauhaus K., Albrecht M., Elvert M., Boetius A. and Widdel F. (2007) In vitro cell growth of  
 918 marine archaeal-bacterial consortia during anaerobic oxidation of methane with sulfate.  
 919 *Environ Microbiol* **9**, 187–196.
- 920 Nigro L. M., Elling F. J., Hinrichs K.-U., Joye S. B. and Teske A. (2020) Microbial ecology and  
 921 biogeochemistry of hypersaline sediments in Orca Basin ed. W. J. Brazelton. *PLoS ONE*  
 922 **15**, e0231676.
- 923 Orcutt B. N., Bradley J. A., Brazelton W. J., Estes E. R., Goordial J. M., Huber J. A., Jones R. M.,  
 924 Mahmoudi N., Marlow J. J., Murdock S. and Pachiadaki M. (2020) Impacts of deep-sea  
 925 mining on microbial ecosystem services. *Limnol Oceanogr* **65**, 1489–1510.
- 926 Oremland R. S. and Polcin S. (1982) Methanogenesis and Sulfate Reduction: Competitive and  
 927 Noncompetitive Substrates in Estuarine Sediments. *Applied and Environmental*  
 928 *Microbiology* **44**.
- 929 Owens J. D., Lyons T. W. and Lowery C. M. (2018) Quantifying the missing sink for global organic  
 930 carbon burial during a Cretaceous oceanic anoxic event. *Earth and Planetary Science*  
 931 *Letters* **499**, 83–94.
- 932 Owens J. D., Reinhard C. T., Rohrsen M., Love G. D. and Lyons T. W. (2016) Empirical links  
 933 between trace metal cycling and marine microbial ecology during a large perturbation  
 934 to Earth’s carbon cycle. *Earth and Planetary Science Letters* **449**, 407–417.
- 935 Paine E. R., Schmid M., Boyd P. W., Diaz-Pulido G. and Hurd C. L. (2021) Rate and fate of  
 936 dissolved organic carbon release by seaweeds: A missing link in the coastal ocean  
 937 carbon cycle ed. C. Pfister. *J. Phycol.* **57**, 1375–1391.
- 938 Porter D., Roychoudhury A. N. and Cowan D. (2007) Dissimilatory sulfate reduction in  
 939 hypersaline coastal pans: Activity across a salinity gradient. *Geochimica et*  
 940 *Cosmochimica Acta* **71**, 5102–5116.
- 941 Raven M. R., Fike D. A., Bradley A. S., Gomes M. L., Owens J. D. and Webb S. A. (2019) Paired  
 942 organic matter and pyrite  $\delta^{34}\text{S}$  records reveal mechanisms of carbon, sulfur, and iron  
 943 cycle disruption during Ocean Anoxic Event 2. *Earth and Planetary Science Letters* **512**,  
 944 27–38.
- 945 Raven M. R., Fike D. A., Gomes M. L., Webb S. M., Bradley A. S. and McClelland H.-L. O. (2018)  
 946 Organic carbon burial during OAE2 driven by changes in the locus of organic matter  
 947 sulfurization. *Nat Commun* **9**, 3409.
- 948 Raven M. R., Keil R. G. and Webb S. M. (2021) Rapid, Concurrent Formation of Organic Sulfur  
 949 and Iron Sulfides During Experimental Sulfurization of Sinking Marine Particles. *Global*  
 950 *Biogeochem Cycles* **35**.

- 951 Raven M. R., Sessions A. L., Adkins J. F. and Thunell R. C. (2016) Rapid organic matter  
952 sulfurization in sinking particles from the Cariaco Basin water column. *Geochimica et*  
953 *Cosmochimica Acta* **190**, 175–190.
- 954 Redfield A. C. (1934) On the Proportions of Organic Derivatives in Sea Water and Their Relation  
955 to the Composition of Plankton.
- 956 Reeburgh W. S. (1976) Methane consumption in Cariaco Trench waters and sediments. *Earth*  
957 *and Planetary Science Letters* **28**, 337–344.
- 958 Reeburgh W. S., Ward B. B., Whalen S. C., Sandbeck K. A., Kilpatrick K. A. and Kerkhof L. J.  
959 (1991) Black Sea methane geochemistry. *Deep Sea Research Part A. Oceanographic*  
960 *Research Papers* **38**, S1189–S1210.
- 961 Ryan W. B. F., Pitman W. C., Major C. O., Shimkus K., Moskalenko V., Jones G. A., Dimitrov P.,  
962 Gorür N., Sakiñç M. and Yüce H. (1997) An abrupt drowning of the Black Sea shelf.  
963 *Marine Geology* **138**, 119–126.
- 964 Schlanger S. O. and Jenkyns H. C. (1976) Cretaceous Oceanic Anoxic Events: Causes and  
965 consequences. *GEOLOGIE EN MIJNBOUW* **55**, 179–184.
- 966 Schmale O., Greinert J. and Rehder G. (2005) Methane emission from high-intensity marine gas  
967 seeps in the Black Sea into the atmosphere: Methane emission from marine gas seeps.  
968 *Geophys. Res. Lett.* **32**, n/a-n/a.
- 969 Schmale O., Haeckel M. and McGinnis D. F. (2011) Response of the Black Sea methane budget  
970 to massive short-term submarine inputs of methane. *Biogeosciences* **8**, 911–918.
- 971 Scranton M. I. (1988) Temporal variations in the methane content of the Cariaco Trench. *Deep*  
972 *Sea Research Part A. Oceanographic Research Papers* **35**, 1511–1523.
- 973 Scranton M. I., Astor Y., Bohrer R., Ho T.-Y. and Muller-Karger F. (2001) Controls on temporal  
974 variability of the geochemistry of the deep Cariaco Basin. *Deep Sea Research Part I:*  
975 *Oceanographic Research Papers* **48**, 1605–1625.
- 976 Scranton M. I., Sayles F. L., Bacon M. P. and Brewer P. G. (1987) Temporal changes in the  
977 hydrography and chemistry of the Cariaco Trench. *Deep Sea Research Part A.*  
978 *Oceanographic Research Papers* **34**, 945–963.
- 979 Sexton P. F., Norris R. D., Wilson P. A., Pälike H., Westerhold T., Röhl U., Bolton C. T. and Gibbs  
980 S. (2011) Eocene global warming events driven by ventilation of oceanic dissolved  
981 organic carbon. *Nature* **471**, 349–352.
- 982 Shah S. R., Joye S. B., Brandes J. A. and McNichol A. P. (2013) Carbon isotopic evidence for  
983 microbial control of carbon supply to Orca Basin at the seawater–brine interface.  
984 *Biogeosciences* **10**, 3175–3183.

- 985 Sheu D.-D. and Presley B. J. (1986) Variations of calcium carbonate, organic carbon and iron  
 986 sulfides in anoxic sediment from the Orca Basin, Gulf of Mexico. *Marine Geology* **70**,  
 987 103–118.
- 988 Shokes R. F., Trabant P. K., Presley B. J. and Reid D. F. (1977) Anoxic, Hypersaline Basin in the  
 989 Northern Gulf of Mexico. *Science* **196**, 1443–1446.
- 990 Siegel D. A., DeVries T., Doney S. C. and Bell T. (2021) Assessing the sequestration time scales of  
 991 some ocean-based carbon dioxide reduction strategies. *Environ. Res. Lett.* **16**, 104003.
- 992 Sinninghe Damsté J. S. and Köster J. (1998) A euxinic southern North Atlantic Ocean during the  
 993 Cenomanian/Turonian oceanic anoxic event. *Earth and Planetary Science Letters* **158**,  
 994 165–173.
- 995 Sinsabaugh R. L. (2010) Phenol oxidase, peroxidase and organic matter dynamics of soil. *Soil*  
 996 *Biology and Biochemistry* **42**, 391–404.
- 997 Stanev E. V., Chtirkova B. and Peneva E. (2021) Geothermal Convection and Double Diffusion  
 998 Based on Profiling Floats in the Black Sea. *Geophysical Research Letters* **48**.
- 999 Starostenko V. I., Rusakov O. M., Shnyukov E. F., Kobolev V. P. and Kutas R. I. (2010) Methane in  
 1000 the northern Black Sea: characterization of its geomorphological and geological  
 1001 environments. *SP* **340**, 57–75.
- 1002 Stewart K., Kassakian S., Krynytzky M., DiJulio D. and Murray J. W. (2007) Oxidic, suboxic, and  
 1003 anoxic conditions in the Black Sea. In *The Black Sea Flood Question: Changes in*  
 1004 *Coastline, Climate, and Human Settlement* (eds. V. Yanko-Hombach, A. S. Gilbert, N.  
 1005 Panin, and P. M. Dolukhanov). Springer Netherlands. pp. 1–21.
- 1006 Trefry J. H. (1984) Distribution and chemistry of manganese, iron, and suspended particulates in  
 1007 Orca Basin. *Geo-Marine Letter* **4**, 125–130.
- 1008 Tribovillard N., Bout-Roumazeilles V., Algeo T., Lyons T. W., Sionneau T., Montero-Serrano J. C.,  
 1009 Riboulleau A. and Baudin F. (2008) Paleodepositional conditions in the Orca Basin as  
 1010 inferred from organic matter and trace metal contents. *Marine Geology* **254**, 62–72.
- 1011 Valentine D. L. (2011) Emerging Topics in Marine Methane Biogeochemistry. *Annu. Rev. Mar.*  
 1012 *Sci.* **3**, 147–171.
- 1013 Van Cappellen P., Viollier E., Roychoudhury A., Clark L., Ingall E., Lowe K. and Dichristina T.  
 1014 (1998) Biogeochemical Cycles of Manganese and Iron at the Oxidic–Anoxic Transition of a  
 1015 Stratified Marine Basin (Orca Basin, Gulf of Mexico). *Environ. Sci. Technol.* **32**, 2931–  
 1016 2939.

- 1017 Wakeham S. G., Lewis C. M., Hopmans E. C., Schouten S. and Sinninghe Damsté J. S. (2003)  
1018 Archaea mediate anaerobic oxidation of methane in deep euxinic waters of the Black  
1019 Sea. *Geochimica et Cosmochimica Acta* **67**, 1359–1374.
- 1020 Ward B. B., Kilpatrick K. A., Novelli P. C. and Scranton M. I. (1987) Methane oxidation and  
1021 methane fluxes in the ocean surface layer and deep anoxic waters. *Nature* **327**, 226–  
1022 229.
- 1023 Wiesenburg D. A., Brooks J. M. and Bernard B. B. (1985) Biogenic hydrocarbon gases and sulfate  
1024 reduction in the Orca Basin brine. *Geochimica et Cosmochimica Acta* **49**, 2069–2080.
- 1025 Young L. Y. and Frazer A. C. (1987) The fate of lignin and lignin-derived compounds in anaerobic  
1026 environments. *Geomicrobiology Journal* **5**, 261–293.
- 1027 Zhang J.-Z. and Millero F. J. (1993) The chemistry of the anoxic waters in the Cariaco Trench.  
1028 *Deep Sea Research Part I: Oceanographic Research Papers* **40**, 1023–1041.
- 1029 Zhuang G.-C., Elling F. J., Nigro L. M., Samarkin V., Joye S. B., Teske A. and Hinrichs K.-U. (2016)  
1030 Multiple evidence for methylotrophic methanogenesis as the dominant methanogenic  
1031 pathway in hypersaline sediments from the Orca Basin, Gulf of Mexico. *Geochimica et*  
1032 *Cosmochimica Acta* **187**, 1–20.
- 1033 Zolotarev V. G., Sochel'nikov, V V and Malovitskiy, Ya P (1979) Heat flow in the Black and  
1034 Mediterranean seas. *Oceanology* **19**, 701–704.
- 1035  
1036  
.....  
1037